

TIME SPECTROMETER FOR THE MEASUREMENT
OF POSITRON LIFETIMES

A Thesis Submitted
in Partial Fulfilment of the the Requirements
for the Degree of
MASTER OF TECHNOLOGY

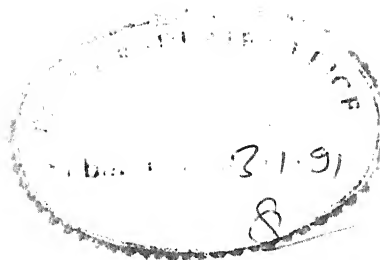
by

ARUN KUMAR CHAKRABORTY

to the

DEPARTMENT OF NUCLEAR ENGINEERING AND TECHNOLOGY
INDIAN INSTITUTE OF TECHNOLOGY KANPUR

JANUARY, 1991



CERTIFICATE

This is to certify that the work presented in this thesis entitled

"TIME SPECTROMETER FOR THE MEASUREMENT OF POSITRON LIFETIMES"

by Arun Kumar Chakraborty has been carried out under my supervision and that this work has not been submitted elsewhere for a degree.

IIT Kanpur.

Jan '91.

A handwritten signature in black ink, appearing to read "R.M. Singru".

(R.M. SINGRU)

(Professor, Dept. of

Physics, IIT Kanpur)

10 APR 1991

CENTRAL LIBRARY
I. I. T., KANPUR

Acc. No. A. 7.890.11
110687

TH
539-7374
C344F

NET- 1991-M-CHA-TIM

ACKNOWLEDEMENTS

I express my deep sense of gratitude towards Professor R.M.Singru for his help and guidance through the course of my M.Tech. thesis work. His continued encouragement has enabled me to complete this work. His helpful suggestions and timely advice has been of great help to me.

I am highly indebted to Dr.U.C.Johri for his endless enthusiasm and constant guidance for my work. Indeed, it has been a great pleasure and privilege for me to have been associated with him during the course of this work.

I am thankful to Prof.K.Sri Ram for the constant source of inspiration and the parental care that he has provided throughout my stay in this institute. Thanks are due, to Prof.A.Sengupta, Dr.M.S.Kalra, Dr.P.Munshi, Dr.V.N.Kulkarni and Dr.S.K.Saha for their helpful company and moral support which made my stay in this institute a pleasure.

I am also thankful to the people in the physics workshop and to the NET staff for the help extended to me.

I wish to record my thanks to Mr.K.M.L.Jha for his assistance through out this work. Also I take this opportunity to thank Mr.P.M.G.Nambissan and Mr.V.S.Subrahmaniam for providing us with the computer programs for data analysis.

My sincere thanks are due to all my friends and well wishers.

I wish to express my deep sense of gratitude towards my parents whose blessings will continue to be a guiding force for my success in every field of life. Finally I wish to offer my deep sense of gratitude to Diptasri who has been my source of inspiration and whose constant encouragement proved invaluable to me in finishing this work.

A.K.CHAKRABORTY.

LIST OF CONTENTS

I) List of Figures	viii
ii) Abstract	vii

CHAPTER

1. INTRODUCTION

1.1 Positron annihilation and positronium formation.	1
1.1.1 Introduction.	1
1.1.2 Lifetime for the 2 photon and 3 photon annihilations.	4
1.1.3 Factors governing positronium formation.	5
1.1.4 Quenching.	6
1.2 Methods for positron annihilation studies.	7
1.2.1. Positron lifetime measurements.	8
1.2.2 Angular correlation measurements.	13
1.2.2.1 Experimental angular correlation measurements.	14
1.2.3 Doppler broadened annihilation line shape.	16
1.2.3.1 Experimental measurement of Doppler broadened line shape.	16

2. EXPERIMENTAL DETAILS.

2.1. Introduction.	21
2.2. Basic setup for measuring lifetime of positrons.	21

2.3. Brief description of each functional unit.

2.3.1. Source.	23
2.3.2. Scintillator.	24
2.3.3. Photomultiplier tube.	24
2.3.4. Photomultiplier base.	25
2.3.5. High voltage supply.	26
2.3.6. Constant fraction differential discriminator.	26
2.3.7. Time-to-pulse-height-converter.	27
2.3.8. Delay cable.	28
2.3.9. Fast coincidence.	29
2.3.10 Time calibrator.	29
2.3.11 Multichannel analyser.	30

2.4. Experimental setting.

2.4.1 Window setting for the CFDD with ^{22}Na .	31
2.4.2. Pulse shape checking.	33

2.5. Performance testing.

2.5.1 Prompt spectrum.	33
2.5.2. Time calibration.	35
2.5.3. Calculation of FWHM from the prompt spectrum.	38
2.5.4. PALT spectrum in teflon.	41

3. DATA ANALYSIS RESULTS AND DISCUSSION.

3.1. Introduction.	42
--------------------	----

3.2. Data analysis.	42
3.2.1 Background.	43
3.2.2. Graphical analysis.	44
3.2.3. Data analysis using computer programs.	44
3.2.3.1. Resolution.	45
3.2.3.2. Positronfit.	45
3.3 Lifetime spectrum data collection and analysis.	46
3.3.1. PALT spectrum in teflon.	47
3.3.2. Lifetime spectrum in annealed copper.	48
3.3.4. Spectrum in a metallic glass sample.	50
3.3.4.1 Amorphous metallic alloys.	50
3.3.4.2. Results of the PALT spectrum in metallic glass.	53
3.4. Discussions.	54
REFERENCES	59
APPENDIX A	

Typical output of the program RESOLUTION.

ABSTRACT

In this work a time spectrometer for measuring the lifetime of positrons in materials has been setup. The coincidence technique used for this purpose is the fast-fast coincidence. The emphasis is on optimising the performance of the time spectrometer. Positron annihilation lifetime (PALT) spectrum has been taken in a metallic glass sample to find the lifetime of the positrons in it.

LIST OF FIGURES

Fig NO.	Caption	Page
1.1	Schematic representation of positron annihilation process.	9
1.2	Schematic diagram of the fast-slow coincidence system used for the lifetime measurement.	10
1.3	Decay scheme of ^{22}Na .	12
1.4	A typical positron lifetime spectrum of metal sodium in semilogarithmic plot.	12
1.5	The vector diagram of the momentum conservation in the 2γ annihilation process.	15
1.6	Block diagram of angular correlation apparatus with long slit geometry for 2γ annihilation radiation.	15
1.7	Typical angular correlation curves in metals (aluminium and copper).	17
1.8	The system for measuring the shape of the Doppler-broadened annihilation line.	17
1.9	Doppler-broadening spectrum.	19
2.1	Block diagram of the time spectrometer using the fast-fast coincidence technique.	22
2.2	Energy spectrum of ^{22}Na and ^{60}Co using plastic scintillator. [19].	32
2.3	Decay scheme of ^{60}Co .	34

2.4	The prompt spectrum of ^{60}Co .	36
2.5	Typical system interconnection for time calibration.	37
2.6	Time calibration line.	39
2.7	PALT spectrum in teflon.	40
3.1	PALT spectrum in annealed copper.	49
3.2	PALT spectrum in metallic glass.	55
3.3	A schematic diagram of time spectrometer using pile up gate.	57

CHAPTER-1.

INTRODUCTION

1.1 POSITRON ANNIHILATION AND POSITRONIUM FORMATION :-

1.1.1 INTRODUCTION

The existence of positrons was predicted by Dirac [1] in 1930 to explain the positive and the negative energy solutions of the relativistic wave equation of the electron. According to his theory, both positive as well as negative energy states are allowed for the electron. The negative energy states are normally completely filled up. If we impart an energy $E \geq 2m_0c^2$ to the electrons in the negative energy states, it would be possible to raise a negative energy electron to a positive energy state, since the gap between the positive and the negative energy states is $2m_0c^2$. Such a transition will mean that a hole has been created in the sea of negative energy electrons. This "hole" behaves, for all practical purposes, as a particle having mass equal to that of an electron but with the charge equal to $+e$, hence the name positron. Similarly if there is a hole in the negative energy sea of electrons, an electron from the positive energy state could fall into the vacant negative energy state and then both electron and the positron disappear, and the equivalent energy $2m_0c^2$ of the electron positron pair appears in the form of electromagnetic radiation (gamma-rays). This process of disappearance of positron electron

pair and production of gamma rays is known as positron annihilation.

After the theoretical predictions of positrons by Dirac these particles were experimentally discovered by Anderson [2] and Blackett and Occhialini [3] in cloud chamber tracks of cosmic ray showers. It was later found that positrons were also emitted by radioactive nuclei undergoing β^+ decay.

It has been theoretically shown that in material medium positron quickly thermalises and comes to rest before annihilating [4,5]. This annihilation results in the emission of one or two or three (or more) photons, the cross section for higher quanta processes are negligible. One photon annihilation occurs only when there is an interaction of the pair with some nucleus or another electron. The most common mode of annihilation is the two- or three-photon mode, however, the number to be emitted and their properties depends on the relative spins of the annihilating particles. It has been found that in order to conserve momentum, energy, parity and other symmetries two photons are emitted when the spins are antiparallel to each other (singlet 1S_0 state) and three photons are emitted when the spins are parallel (triplet 3S_1 state). In case of singlet state annihilation each photon carries an energy equal to $m_0c^2 \sim 511$ keV and are emitted at an exact angle of 180° to each other, (these

properties are valid only for the situation where the annihilating pair is at rest). In the case of triplet state annihilation the total energy , $2m_0c^2 \sim 1.022$ Mev, of the annihilating pair is shared by the three photons and these are emitted in one plane with the restriction that no two of them will lie in the same half plane .

The annihilation process described above is known as a direct process, where there is no formation of a bound state between the electron and the positron . However electron and positron can form a bound atomic system and annihilate from this bound state . This bound state , known as positronium atom , is a quasistatic system having a structure similar to the hydrogen atom , the proton nucleus being substituted by a positron nucleus. The possible existence of such a system was suggested by Ruark [6].

In comparison to the hydrogen atom the metastable positronium has a reduced mass of $1/2 m_0$ (m_0 is the rest mass of the electron). Since the energy of the n^{th} level is

$$E_n = - \frac{m_0 e^4}{4n^2 \hbar^2} \quad (1)$$

the energy levels in the positronium atom is reduced by a factor of two in comparison to the hydrogen atom.

The following properties can therefore be inferred about the positronium atoms :-

- i) the ionisation potential is 6.8 eV ,
- ii) the Bohr radii are about twice that of hydrogen atom,
- iii) the first excited state has an energy equal to 5.1 eV ,
- iv) the wavelength of Lyman α line is 2430°\AA .

The positronium atom can be formed either in a singlet or in a triplet state depending upon whether the relative spins of positron and electron are parallel or antiparallel. The para state decays into three photons whereas the ortho state decays into two photons . In the ground state positronium is an admixture of the ortho (3S_1) and para (1S_0) states in the ratio 3:1 and we have

$$Ps = 3/4 (o-Ps) + 1/4 (p-Ps) \quad (2).$$

Ps, o & p refer to the positronium and ortho and para states respectively .

When positronium is formed in excited states ($l > 0$) it decays to the ground state ($l=0$) by optical deexcitation and then annihilates into two or three photons .

1.1.2 Lifetimes for the 2 photon and 3 photon annihilations :

- 1) Two photon annihilation process ;

Dirac [7] calculated the cross section for such a process in the non-relativistic limit , $v \ll c$, (where v is the velocity of the positron and c is the velocity of light) to be

$$\sigma_{2\gamma} = \frac{\pi r_0^2 c}{v} \quad (3)$$

where r_0 is the classical electron radius .

For such a process he obtained the mean lifetime to be

$$\tau_1 = 1.25 * 10^{-10} \text{ sec .} \quad (4)$$

11) Three photon annihilation process ;

The mean life of o-ps state was calculated by Ore & Powell [8] , who found that the ratio of the mean lives for 2γ to 3γ annihilations was

$$\frac{\tau_1(2\gamma)}{\tau_3(3\gamma)} = \frac{4}{9\pi} (\pi^2 - 9)\alpha \quad (5)$$

where α is the fine structure constant ;

$$\text{Thus } \tau_3(3\gamma) = 1.4 * 10^{-7} \text{ sec.} \quad (6)$$

The equations (4) and (5) when compared reveal that the para state of positronium decays 1115 times faster than the ortho state .

1.1.3 Factors governing positronium formation .

Positronium formation in a medium depends upon many factors like the electron density , space available in the medium to accomodate positronium atoms etc. . Experimental evidence suggests that positronium formation is more probable in molecular materials , liquids, amorphous-solids , gases and disordered systems ; whereas it is not formed in metals and ionic crystals . In case of metals the large electron density makes the direct annihilation process the most probable process . In ionic crystals their formation is

energetically not favourable. In case of liquids, disordered systems and amorphous-solids there is enough room i.e free, volume available that makes the formation of positronium more possible in these compounds .

Apart from these restrictions , the energy of the positrons also plays a significant role in deciding whether positronium formation is possible or not .

1.1.4 Quenching.

We have seen that the decay rate for the 3γ annihilation process is less than the 2γ process , however , during collisions of the positronium with the surrounding medium , the state of positronium may change from ortho to para state, which results in a faster decay by a 2γ annihilation . All such process which bring about this conversion of ortho-positronium to para-positronium is known as quenching .

There are four ways in which this quenching may occur :-

1) Spin-flip quenching :-

In this process the spin of ortho positronium is changed due to scattering with molecules of the medium , the ortho positronium is thereby converted to para positronium . Statistically the probability of this process is very small.

11) Pick-off quenching :-

During scattering with molecules , the positron of

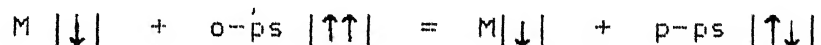
ortho positronium sometimes annihilate with some electrons of the surrounding matter in such a way that the spins of the electron in the surrounding matter and that of the positron are antiparallel, i.e., in the singlet state. This process is known as pick-off quenching. The pick-off rate depends on the time spent by the electrons in sufficient overlap with the molecular electronic orbital. Green and Lee [9] calculated this rate to be $2 \times 10^9 \text{ sec}^{-1}$ and therefore the mean life τ_2 to be of the order of 10^{-9} sec .

iii) Paramagnetic quenching :-

There are two types of paramagnetic quenching ;

a) Direct exchange (spin flip due to unpaired electron) -

In this process the unpaired electron of the paramagnetic molecule replaces an electron of the ortho positronium such that it always decays via para positronium formation,



b) Without spin flip -

In this process the conversion to para positronium results without any change in the spin of the colliding molecule.

1.2 METHODS FOR POSITRON ANNIHILATION STUDIES

The information about the interaction of the positrons with matter is carried by the annihilation gamma rays. A study of these gamma rays enables us to understand the annihilation

process Fig. 1.1 depicts the three processes. Generally the following three types of measurements are performed to study positron annihilation in matter :-

- i) Positron lifetime measurements .
- ii) The angular correlation between the two photons in the $\gamma\gamma$ annihilation process .
- iv) Doppler broadening of annihilation radiation .

1.2.1 POSITRON LIFETIME MEASUREMENTS.

From the non-relativistic limit of $\gamma\gamma$ annihilation cross-section given by Dirac [7] in 1930 , the annihilation rate is obtained as :

$$\lambda = \pi r_0^2 c n_e \quad (7)$$

where r_0 is the classical electron radius , and

n_e is the electron density at the annihilation site.

Thus measuring λ , the inverse of which is the lifetime τ , one gets the value of n_e encountered by the positron . This implies that positron serves as a probe to the electron density in a medium .

The coincidence technique (fast-fast or slow-fast) is used to measure the lifetime . The block diagram of Fig. 1.2 illustrates the slow-fast system along with the source-sample geometry .

The source chosen is usually the radionuclide ^{22}Na with a strength of the order of 10 μCi , it is sandwiched between

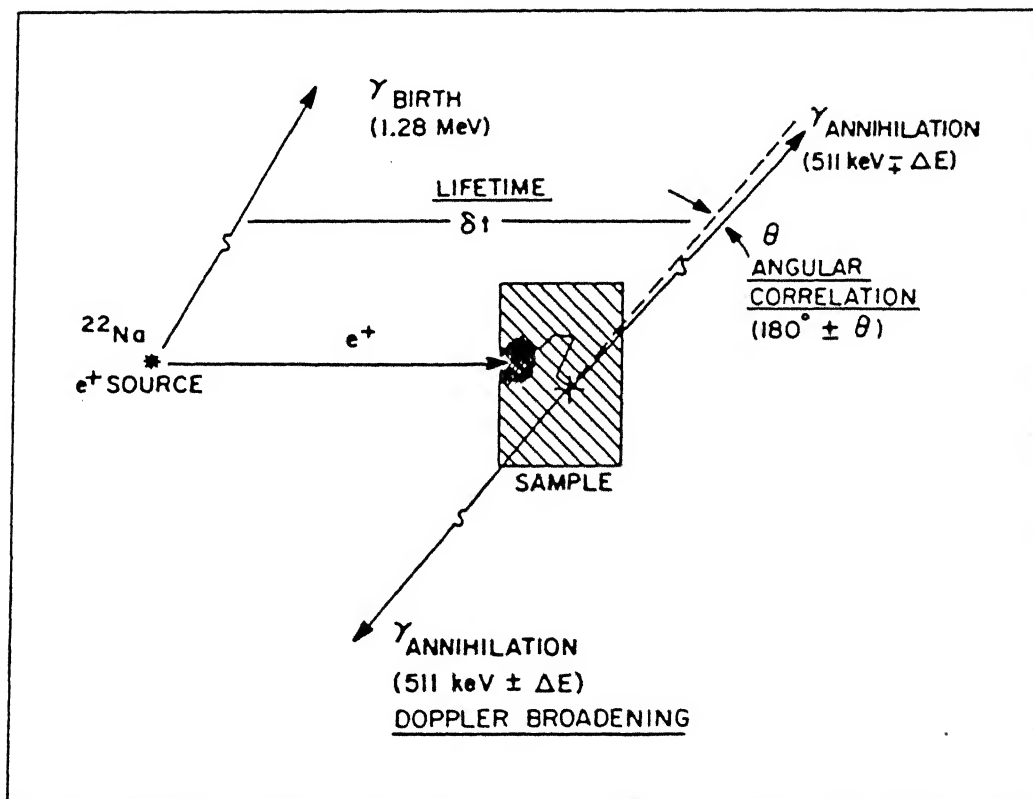


Fig.1.1. Schematic representation of positron annihilation. The basis for the three experimental techniques i) lifetime ii) angular correlation and iii) Doppler broadening are depicted here. [10].

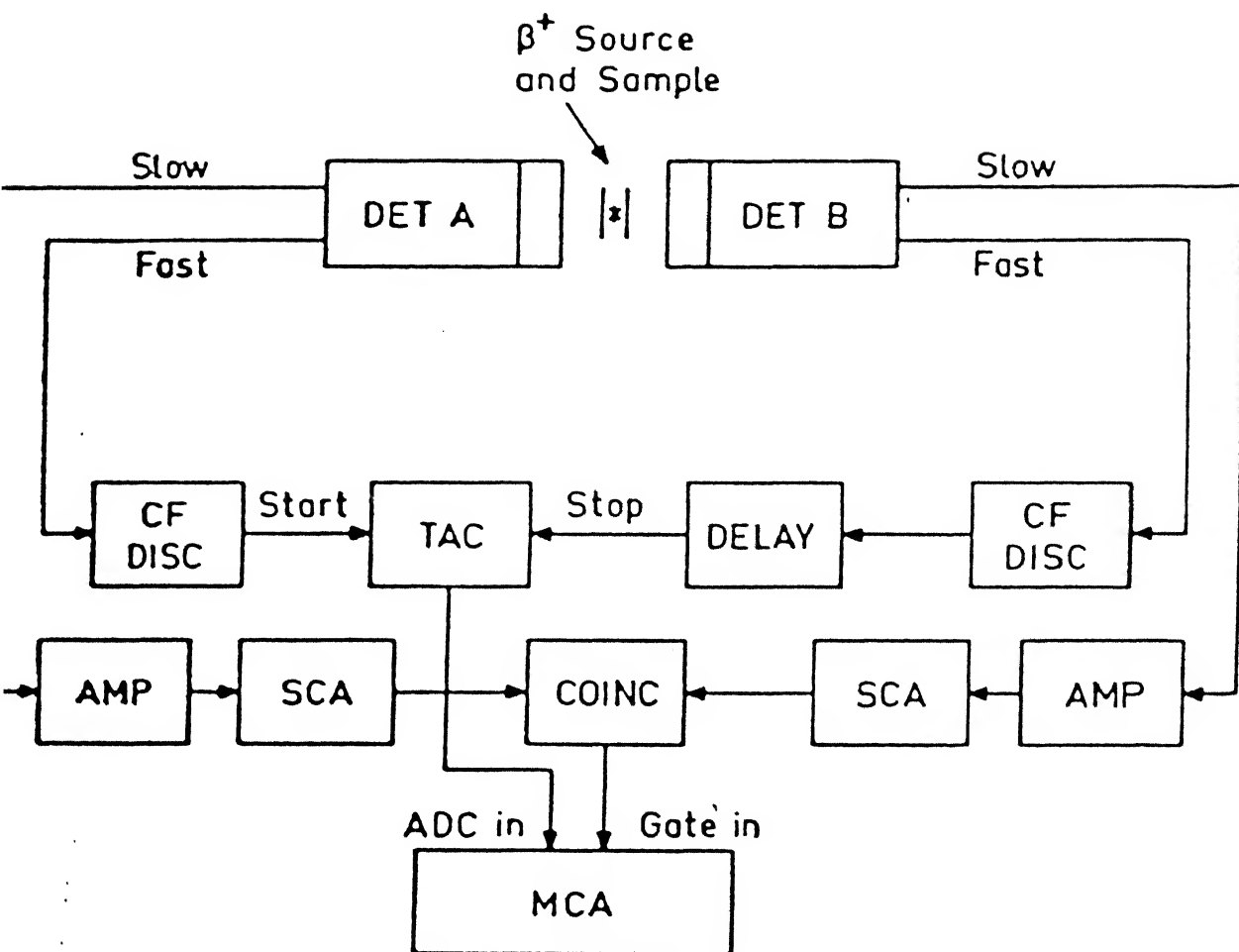


Fig. 1.2. Schematic diagram of the fast-slow coincidence system used for the lifetime measurement. [11].

the two identical samples to be investigated . The positron implantation ranges are generally of the order of $100\mu\text{m}$ to $200\mu\text{m}$, so the sample thickness should exceed $250\mu\text{m}$ to stop all injected positrons .

The radionuclide ^{22}Na , whose decay scheme is shown in Fig.1.3, decays to ground state through the emission of a positron and a 1.276 Mev gamma ray . Since the two emissions are separated by a time interval of the order of 10^{-11} sec. , the 1.276 Mev gamma ray can be considered to be simultaneously emitted with the positron . The detection of this 1.276 Mev gamma ray marks the birth of the positron . This is used as the start signal in the time-to-pulse-height converter, (TPHC). When the positrons annihilate in a singlet state with an electron in the medium , two gamma rays of equal energy 0.51 Mev each are emitted . Detection of any one of these gamma rays marks the annihilation of positron . This is used as a stop signal in the TPHC. The time difference between the detection of the 1.276 Mev gamma ray and the 0.51 Mev gamma ray gives the lifetime of the positron .

In this slow-fast coincidence method, the fast channel is used to establish the time difference δt , while the slow channel is used to drive a linear gate to the multichannel analyser (MCA) using energy selection .

A typical-lifetime spectrum is shown in Fig.1.4.

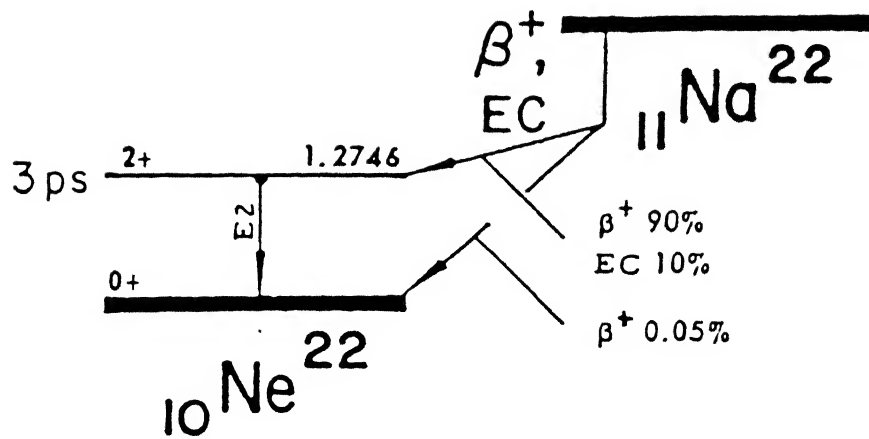


Fig.1.3. Decay scheme of ^{22}Na .

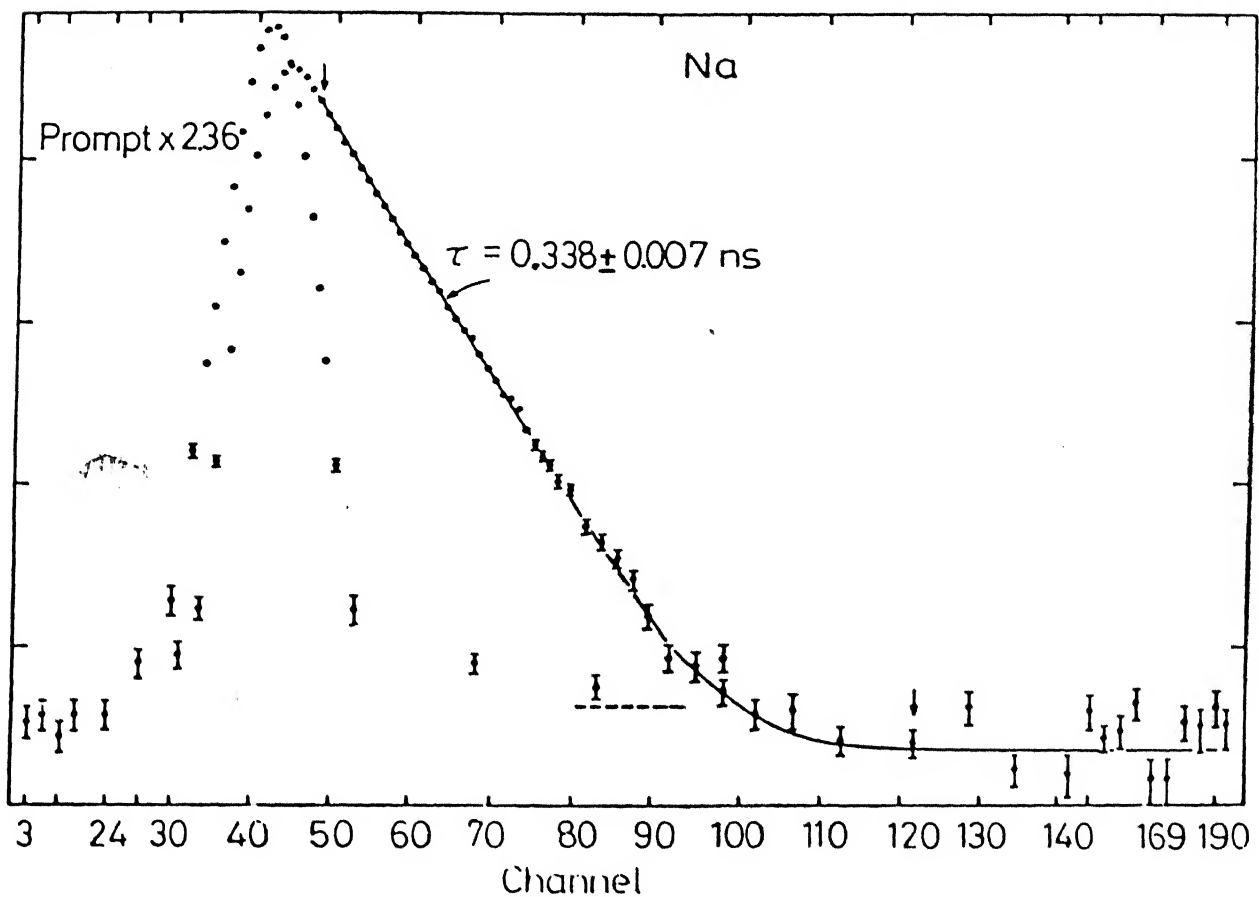


Fig.1.4. A typical positron lifetime spectrum of metal sodium in semilogarithmic plot. The prompt curve represents the instrumental resolution. [12].

1.2.2 ANGULAR CORRELATION MEASUREMENTS .

It has been stated earlier that the annihilation photon energy is $m_0 c^2 \simeq 0.51 \text{ Mev}$ each in case of a two-photon annihilation process and the photons are directed in exactly opposite directions, (i.e. 180° apart), in the centre of mass frame. However if the annihilating pair has a non-zero value of momentum the two annihilating pairs will deviate from collinearity in the laboratory frame, although in the centre of mass frame they will continue to be exactly 180° apart. It is known, that electrons in solids have a continuous momentum distribution with the maximum momentum being the Fermi momentum k_F . Due to this momentum distribution the two annihilating photons will deviate from collinearity. Referring to Fig. (1.5) this value is

$$\theta \simeq \frac{p_T}{m_0 c} \quad (8)$$

where $(180^\circ - \theta)$ is the angle between the photons in the laboratory frame; and

p_T is the momentum component of the electron positron pair transverse to the photon emission direction.

As the momentum of a thermalised positron is zero, the measured angular momentum curves describe the momentum distribution of annihilated electrons in matter.

1.2.2.1 EXPERIMENTAL ANGULAR CORRELATION MEASUREMENTS:-

The block diagram given in Fig.1.6 describes a typical γ annihilation photon angular correlation setup. Positron sources of the type ^{22}Na or ^{58}Co are usually used with an activity higher than 10 mCi. Positrons from the source, kept few millimeters away from the specimen, penetrate into the sample and annihilate there. The annihilation photons are detected in coincidence by NaI scintillation counters. The instrumental angular resolution is typically of the order of 1 mrad or less depending upon the efficiency desired. The coincidence counting is done as a function of θ , where the angle θ is varied mechanically in small steps. The single channel analysers (SCA) are set to accept for 511 keV photons only. Because of the small angular deviation to be measured, the distance between the detectors must be several meters.

The counting rate in angular correlation is given by :

$$N(\theta_z) = c \int_{-\alpha}^{\alpha} \int_{-\alpha}^{\alpha} dp_x dp_y \rho(p_x, p_y, \theta_z m_0 c) \quad (9)$$

where $\rho(p_x, p_y, \theta_z m_0 c)$ is the momentum distribution of the annihilating positron-electron pair in the sample medium.

It has been shown by Farrell [15] that the shape of the angular distribution curve for positron annihilation in free electron gas is an inverted parabola. Experimentally some tails are also observed. The parabolic part is considered to

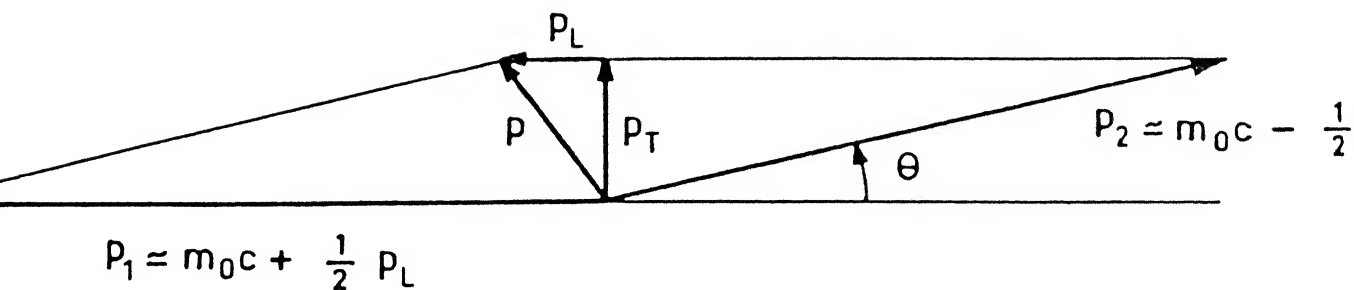


Fig.1.5. The vector diagram of the momentum conservation in the 2γ annihilation process. The momentum of the annihilating pair is denoted by P , subscripts L and T refer to longitudinal and transverse components respectively. [13].

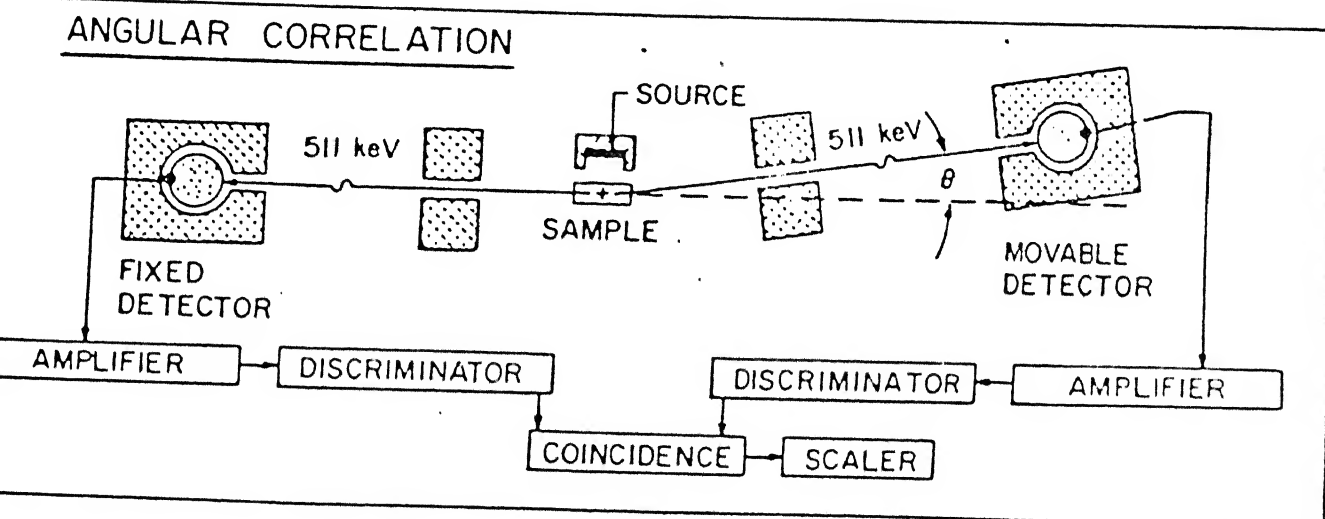


Fig.1.6. Block diagram of angular correlation apparatus with long slit geometry for 2γ annihilation radiation. [14].

arise due to annihilation with valence electrons, and the broader, roughly Gaussian shaped component, is considered to arise due to annihilations with core electrons having higher momentum values .

A typical angular correlation curve is shown in Fig.1.7.

The momentum distribution of the valence electron has a cut-off at the Fermi surface and the corresponding momentum value $\theta_{F0}c$ can be directly obtained from the intersection of the two components , mentioned above .

1.2.3 DOPPLER BROADENED ANNIHILATION LINESHAPE :

The non-zero momentum of the positron-electron pair also causes a Doppler shift in the energy of the annihilation photons measured in the laboratory system .

The frequency shift is $\Delta\nu/\nu = v_L/c$,
where , v_L is the longitudinal centre of mass velocity of the pair i.e $P_L / 2m$,

as the energy of the photon is proportional to its frequency we get a Doppler shift (ref Fig.1.5) at the energy m_0c^2 as

$$\Delta E = (v_L / c) E = c P_L / 2 \quad (10)$$

1.2.3.1

EXPERIMENTAL MEASUREMENT OF DOPPLER BROADENED LINESHAPE.

A high resolution solid state detector is used to study the lineshape. As shown in Fig.1.8 the annihilation is

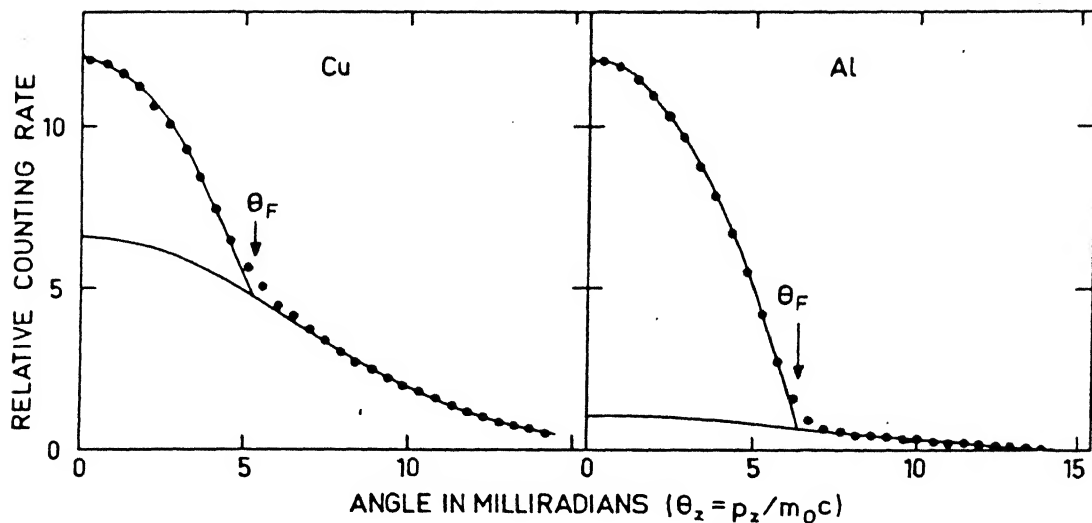


Fig.1.7. Typical angular correlation curves in metals (aluminium and copper). The inverted parabolas are due to free electrons and the Gaussian parts are due to core electrons. [16].

β^+ Source
and Sample

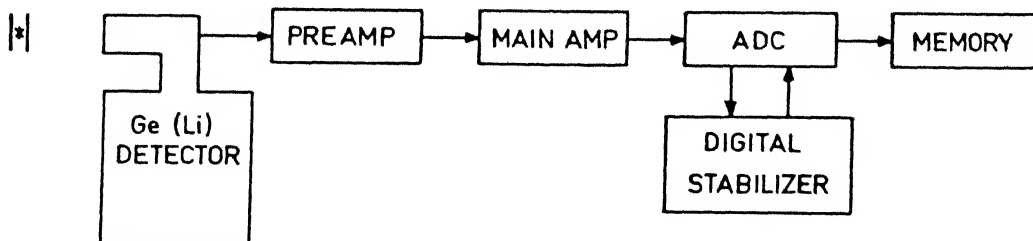


Fig.1.8. The system for measuring the shape of the Doppler-broadened annihilation line. [17].

detected by a Ge(Li) detector . The amplified signal is fed to an on-line computer via an analog-to-digital converter (ADC). The sample-source configuration is similar to that used in a lifetime experiment , however as there is no necessity of detecting a coincident birth γ ray , sources like ^{68}Ge or ^{58}Co may also be used.

The resolution of the detectors used are about 1 keV at 511 keV . This, in terms of angular resolution is only 4 mrad, which is poor in comparison to resolution for angular correlation experiment (0.2 mrad) . However in most experiments the details of electron momentum information is not required and therefore the limitation in resolution can be compensated by the considerable increase (about 100 times) available in statistical efficiency, due to the use of highly efficient detectors. As such Doppler broadening technique is popular for defect studies in materials in which the changing state (either concentration or type) of the defect population is being monitored, since a statistically significant spectrum can be obtained in less than one hour.

A typical Doppler broadened spectrum is shown in Fig.1.9. Lineshape parameter I_V and I_C are defined to emphasize positron annihilation with valence and core electron respectively. I_V and I_C are measured with respect to the total area under the spectrum .

I_V is defined for a region approximately 0.5 keV or 2 mrad

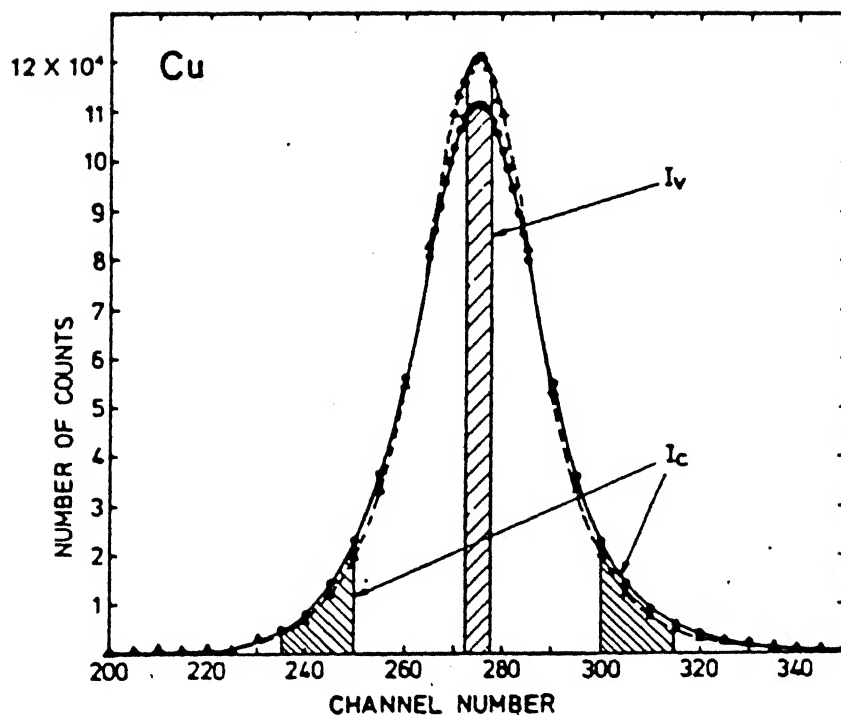


Fig.1.9. Doppler-broadening spectra from annealed (---) and electron irradiated (Δ) copper. Two lineshape parameters I_v and I_c are indicated. The Doppler-broadened line is centered at 511 keV and the width of each channel is 0.01 keV. [18].

CHAPTER-2.

EXPERIMENTAL DETAILS

2.1 INTRODUCTION .

This chapter describes the experimental details of our positron lifetime spectrometer used for the measurement of lifetime of positrons. A brief description of each functional unit is also given.

2.2 BASIC SET-UP FOR MEASURING LIFETIME OF POSITRONS.

In the present work the fast-fast coincidence technique is used for measuring the lifetime of positrons. The block diagram of the set-up used is given in Fig.2.1. In the fast-fast coincidence technique, the fast, constant fraction differential discriminator performs the function of timing as well as that of energy selection in a single width module. The counting rate in this method is higher than that achieved in the slow-fast method.

In our experiment a single high voltage unit is used to drive the two photomultiplier tubes (PMT). The fast anode pulses from the two PMT bases are fed into the input of the constant fraction differential discriminator (CFDD) which then carries out the energy and time selection. The timing information are carried by the timing outputs, and they are used as the start and stop signals for the

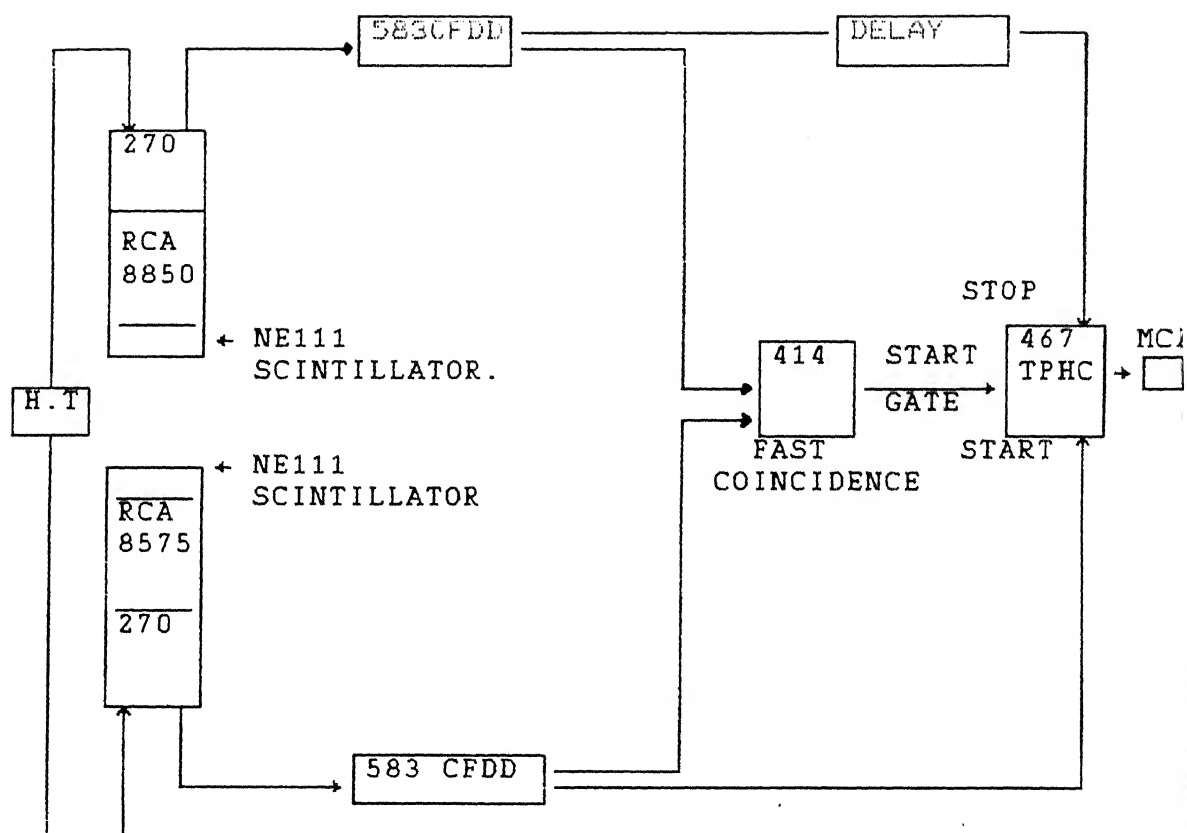


Fig. 2.1. Block diagram of the time spectrometer using the fast-fast coincidence technique.

time-to-pulse-height converter (TPHC), corresponding to the γ ray energies of 1.28 MeV and 0.51 MeV respectively.

The information regarding the energy of the pulse is carried by the SCA output of CFDD. The energy selection is done by setting the discriminator level of the CFDD to accept pulses which are in an upper 30% of the Compton distribution of the corresponding pulses. The determination of the Compton edge is done by the window setting of the CFDD, this process is described later. The SCA outputs are fed into a fast coincidence unit which delivers an output only when the two pulses arrive at its input within a time $2\tau_0$, known as the resolving time.

This fast coincidence unit output is used to gate the TPHC output. This TPHC output is fed to a multi-channel analyser (MCA). This MCA records the lifetime spectrum.

2.3 BRIEF DESCRIPTION OF EACH FUNCTIONAL UNIT :

2.3.1 SOURCE

The source used in the experiment is the radionuclide ^{22}Na . The decay scheme of this source was given in Fig.1.3. The half life of the source is 2.6 years and the maximum energy of the positrons is 0.545 MeV. The 1.28 MeV γ ray is used as the start signal, while the stop signal is furnished by the 0.51 MeV annihilation γ ray.

2.3.2 SCINTILLATOR.

The scintillators used in this experiment are plastic NE111, of cylindrical shape, having a size of 25 mm diameter and 30 mm height. The surface of each crystal and their top face (nearer the source) is painted with a white reflecting

paint supplied by Nuclear Enterprises Ltd..The function of the scintillator is to convert the kinetic energy of the pulse incident on it into detectable light with high scintillation efficiency. For propagation of fast signal pulses the decay time of the induced luminescence should be short. The index of refraction of the scintillator is 1.58 and this is necessary for good optical coupling with the PMT's photocathode. The fluorescence process arises from transitions in the energy level structure of a single molecule of the crystal.

In the case of NE111 the light output is 55% , the decay time is 1.7 ns and the wavelength of light emitted is 375 \AA .

2.3.3 PHOTOMULTIPLIER TUBE.

The extremely weak light output from the scintillators is converted into large electrical signal in a photomultiplier tube. The two tubes used in this experiment are the RCA 8575 (used in the start channel) and the RCA 8850 (used in the stop channel). The light from the scintillators is fed into

the photosensitive layer known as the photocathode, which converts the light photons into low energy electrons. These electrons are multiplied (in number) in the electron multiplier section (consisting of dynodes) to about 8×10^6 electrons at a voltage of 2000 volts, which is the overall voltage. These linear tubes are of 53.3 mm maximum diameter, and of length 145 mm. The maximum voltage that can be applied is 3 kV, but in this experiment a high voltage equal to 1.9 kV was applied. The transit time, which is the average time difference between the arrival of a photon at the photocathode and the subsequent electron burst at the anode, is ≤ 2.5 ns (as quoted by the manufacturer) at the maximum voltage.

In order to avoid the effects of stray magnetic fields on the trajectory of the electrons in the PMT (the average energy of electrons in the tube is ~ 100 eV), a magnetic shield in the form of a cylinder made of mu-metal is fitted closely around the glass envelope of the PMT.

2.3.4 PHOTOMULTIPLIER BASE.

The electrical signal obtained from the photomultiplier tube is fed into the photomultiplier base (ORTEC MODEL 270). The purpose of the PMT base is to accomodate the PMT and to distribute the operating voltages to all its dynodes and derive signal from its anode and a selected dynode.

The anode signal from this base is fed into the CFDD input

for timing purposes. This signal is a negative timing signal, nominally -16 mA on a 50 Ω load having a width ~ 6 ns and a rise time < 2.5 ns.

2.3.5 HIGH VOLTAGE SUPPLY.

The high voltage to the PMT is provided by a single unit (CANBERRA MODEL 3002). It can supply high voltage upto 3 kV (both positive as well as negative), with 10 mA output current capability. In this experiment a high voltage of -1.9 kV is applied.

2.3.6 CONSTANT FRACTION DIFFERENTIAL DISCRIMINATOR. (CFDD).

The CFDD used in this experiment is ORTEC MODEL 583. It is a single width NIM module that generates accurate timing output signals. It is used as a fast single channel analyser for the anode signals from the fast PMTs, from where the input pulses are accepted in the range of 0 to -10 V. The discriminator range in the CFDD varies from -30 mV to -5 V. The outputs of the CFDD utilized in the experiment are the timing output, which is a NIM standard fast negative logic pulse and the positive SCA output, which is a NIM standard slow positive logic pulse and occurs simultaneously with the timing output.

The output logic pulse which is 20 ns wide and 1 V in height produced on the basis of the constant fraction

principle, where the input signal from the fast photomultiplier is delayed and a fraction of the undelayed pulse is subtracted from it. The zero crossing point of the bipolar signal thus generated is used to produce timing information via an output logic pulse. The delay in the input signal depends on the length of the delay cable used externally, where the approximate calibration of the delay used is,

$$\text{delay} = 0.7 \text{ ns} + \text{the delay of the external cable.} \quad (1)$$

2.3.7 TIME-TO-PULSE-HEIGHT CONVERTER (TPHC).

The TPHC used here is a double width NIM standard ORTEC MODEL 467. The purpose of the TPHC is to measure the time interval between the leading edge of the logic pulses at its start and stop input. The timing outputs of the CFDD are fed to the start and the stop inputs of the TPHC. In its output the TPHC generates an analog pulse that is proportional to the measured time interval, the peak pulse height can be upto +10 V. The rise time of the output pulses are < 500 ns and their width is internally adjustable from 1.0 μ s to 2.5 μ s. The full scale time ranges can be selected from 50 μ s to 80 ns, in this experiment the range scale was selected as 100 ns.

The TPHC output pulse has a peak amplitude that is proportional to the ratio of the measured time interval

(between the start and the stop pulse) to the selected full scale interval, and the range of these pulses is from 0 to +10 V.

In the experiment the start and the stop inputs are delayed by 100 ns and 130 ns respectively for proper coincidence requirement. The input gate for the start circuit is operated in the coincidence mode. The gating is done by the output pulse from the coincidence unit whose output must be a logic pulse, with the convention :- logic 0 for $< +2$ V pulse and logic 1 for $> +2$ V pulse. The gate signal must occur about 10 ns before the start input pulse.

Basically the conversion of the start to stop interval to pulse height is carried out as follows. The start pulse sets the memory of a tunnel diode to the ONE state, the stop pulse resets the memory to the ZERO state. A capacitor is charged in the ONE state interval and the voltage across this gives the pulse height. The output from the TPHC is directly fed into the MCA. The calibration of the TPHC which gives the time per channel in the MCA is done using a time calibrator (ORTEC MODEL 462) described later.

2.3.8 DELAY CABLE.

The delay in the start and the stop channel is introduced using the RG-58 cable which introduces a propagation delay equal to 5.05 ns per meter.

For example, a 30 ns delay is introduced by a 5.94 meter long cable.

2.3.9 FAST COINCIDENCE.

The fast coincidence between the two SCA outputs of the CFDD is carried out by using a double width NIM standard ORTEC MODEL 414 fast coincidence unit. The module allows coincidence between any two or three input signals, in the experiment coincidence between any two input signals was used. The fast coincidence is carried out using an AND circuitry. The resolving time (2τ) between the two input signals can be varied in the module in discrete steps from 10 ns to 110 ns, in the experiment it was maintained fixed between 40 ns and 50 ns. The inputs of this module accepts logic pulses which are positive, 2 V in height and of minimum 20 ns width. The output is a logic pulse of minimum height 4 V and has a 500 ns full width at half maxima (FWHM).

2.3.10 TIME CALIBRATOR.

The calibration (time per channel) of the TPHC was done by using the time calibrator (ORTEC MODEL 462). The function of this double width NIM standard module is that it generates fast negative logic pulses at precise time intervals that can be fed into the start and stop inputs of the TPHC. The time base is a crystal controlled 100 MHz oscillator. Each pair of start and stop pulses are exactly N integral time intervals apart, where N is an integer and is a multiple (2 or more) of

the selected period set in the module. A range switch limits the maximum multiple N , the selected range can be varied from 80 ns to 81.92 μ s. The period can be varied at 11 steps from 10 ns to 10.24 μ s, the range must be set to be greater than the period. The pulse rate from the oscillator can be varied continuously from 100 to 50,000 counts per sec.

In the experiment a 10 ns period was selected to calibrate the TPHC.

2.3. 11 MULTICHANNEL ANALYSER.

The output available from the TPHC is analysed by Nuclear data Model ND65 Multichannel analyser (MCA), used in the pulse height analysis mode. The basic function of the MCA is to gather and store in a histogram memory the spectral data acquired from the data acquisition system.

There are two modes of data acquisition in an MCA, they are 1) the pulse height analysis mode and 11) the multichannel scaling mode. The desired spectrum is accumulated by measuring the amplitude of each input event by converting it into a number or channel address that is proportional to the pulse height and storing the information in a memory composed of individual channels. The count value of each channel is equal to the total number of pulses processed whose amplitudes correspond to the channel number. The maximum number of counts a channel can store is 10^6 . The conversion of the analog signal (the pulse amplitude) into a

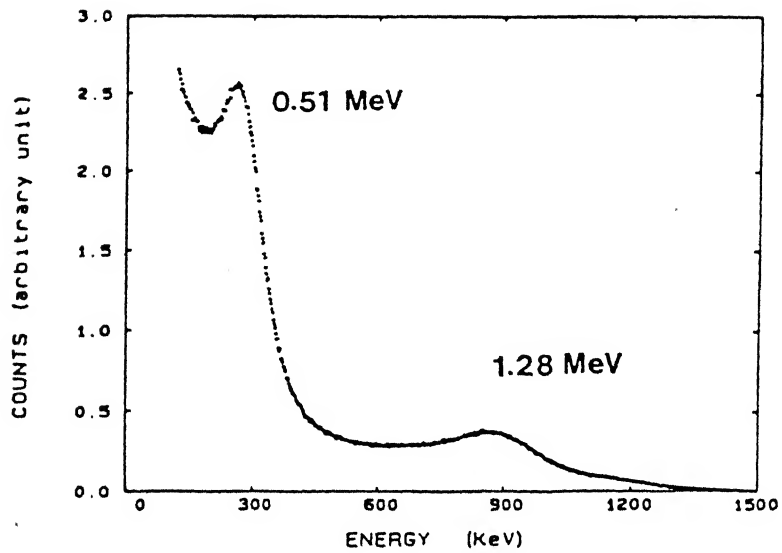
digital number is done in an analog-to-digital converter (ADC) in the MCA. The output of the ADC is stored in a computer type memory which has as many addresses as the maximum number of channels the spectrum is recorded in. The channel numbers range from 256 to 8191, the increase is in steps of multiple of two. In the experiment the number of channels used were mostly 2048 but 1024 channels were also used at times.

2.4. EXPERIMENTAL SETTING.

2.4.1. WINDOW SETTING FOR THE CFDD WITH ^{22}Na .

In the experimental setup for measuring the positron annihilation lifetime (PALT) in any medium, the selection of the start and the stop channel is governed by the setting of the CFDD discriminator window. The setting of window means adjusting the CFDD to receive the γ rays of a particular energy range. To achieve this the singles spectrum is recorded by scanning the whole spectrum range of ^{22}Na with the help of a scaler keeping the difference (ΔE) between the two levels as 0.04 V. The count vs. different lower level (E) readings is plotted on a semi-log graph and is of the type shown in Fig.2.2.. The graph shows a Compton distribution corresponding to the energies 0.51 MeV and 1.28 MeV. The scintillators being organic in nature no photopeaks can be seen.

^{22}Na energy spectrum.



^{60}Co energy spectrum.

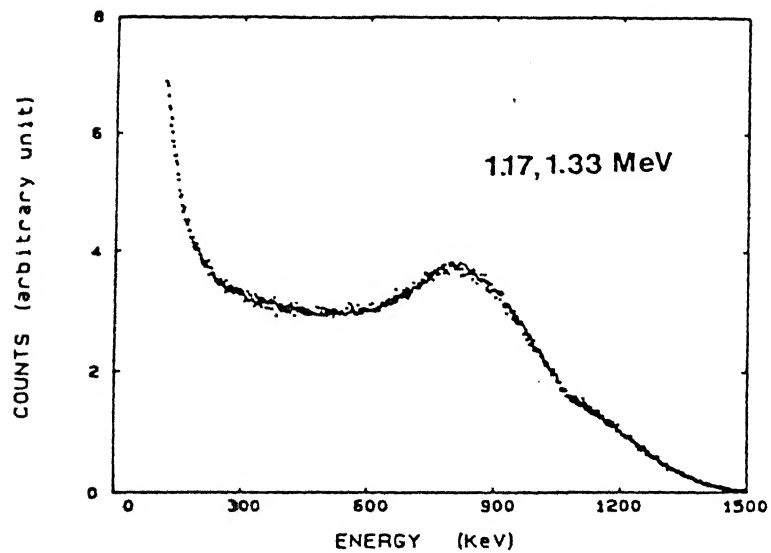


Fig.2.2. Energy spectrum of ^{22}Na and ^{60}Co using plastic scintillator. [19].

The window setting is done by setting one of the CFDD bias to accept the upper 30% of the Compton distribution of the 0.51 MeV and setting the other CFDD bias to accept upper 30% of the Compton distribution corresponding to the 1.28 MeV γ ray.

2.4.2. PULSE SHAPE CHECKING.

After all the connections in the setup were ready the pulses from the PMT base, CFDD timing output, CFDD SCA output, fast coincidence output and the output from the TPHC were checked to ensure that they were in conformity with the given specifications. The standard pulse shapes were referred from the manuals of the modules concerned.

2.5. PERFORMANCE TESTING.

2.5.1. PROMPT SPECTRUM.

One of the first major task in setting up of a lifetime spectrometer is to examine (and improve) its prompt spectrum.

After the window selection is done, the ^{22}Na source is replaced by a ^{60}Co source. The ^{60}Co radionuclide whose decay scheme is shown in Fig.2.3. is known to emit two γ rays of energies 1.17 MeV and 1.33 MeV respectively, and are separated by a time difference of $\sim 10^{-12}$ secs..This can be

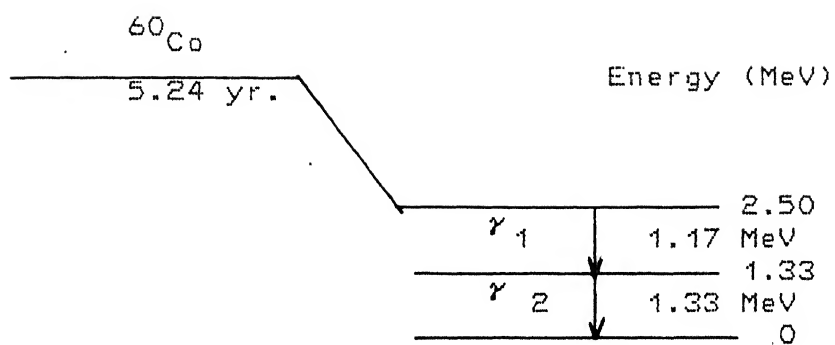
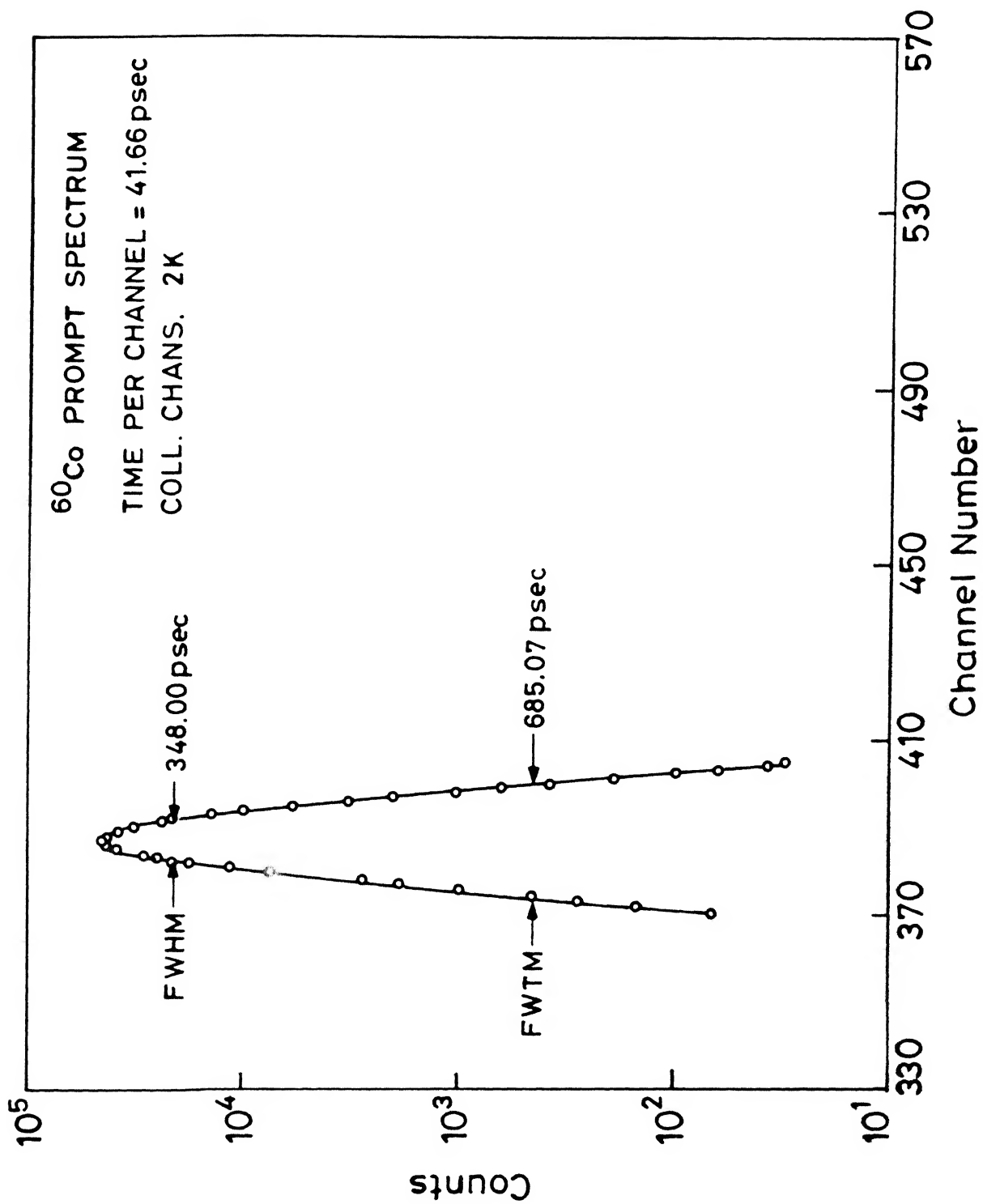


Fig.2.3. Decay scheme of ^{60}Co .

considered to be almost simultaneous in comparison to the instrumental resolution. The record of the time distribution is known as the 'prompt spectrum'. The full width at half maximum (FWHM) of the prompt spectrum indicates how accurately the prompt events of ^{60}Co source can be measured by the time spectrometer. Due to the use of a 30 ns relative delay in the stop arm, the time spectrum at the 30 ns time is recorded as the t_0 channel. Ideally the spectrum should be of a delta function type, however the nature of the detection process introduces uncertainties on either side of $t_0 = 30$ ns. This time spectrum which is approximately Gaussian in nature will give an indication of the intrinsic ability or the timing resolution of the spectrometer for measuring the time spectra. The prompt spectrum obtained with ^{60}Co is shown in Fig.2.4..

2.5.2 TIME CALIBRATION.

After recording the prompt spectrum due to ^{60}Co its FWHM value is to be determined. This calculation requires the knowledge of time calibration (in ns) per channel of the recorded spectrum. To determine this the time calibrator is connected to the TPHC as shown in Fig.2.5.. The output of the TPHC (which shows peaks at regular time interval corresponding to the set period in the time calibrator) is recorded in an MCA. A graph of time interval i.e the period



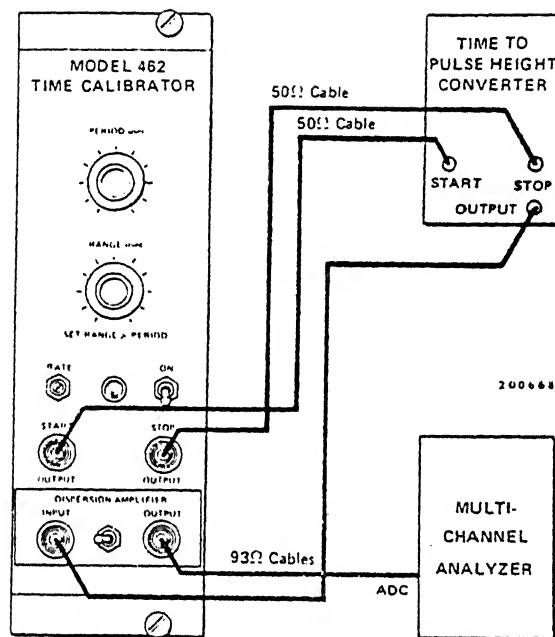


Fig. 2.5. Typical system interconnection for time calibration.

in the time calibrator vs channel number is drawn by the least square fit method as shown in Fig.2.6.. The slope of this graph gives the time per channel. In our experiment the time calibration was 41.66 ns/channel when 2K MCA channels were used and 83.22 ns/channel when 1K MCA channels were used.

2.5.3. CALCULATION OF FWHM FROM THE PROMPT SPECTRUM.

After the time calibration is noted, the next step is to calculate the FWHM using the time calibration. The width in number of channels of the position in the graph where the count is half the peak count multiplied by the time calibration gives the value of FWHM.

It should be pointed out here that the prompt spectrum was taken with different external delay cable lengths (connected at the front pannel of the CFDD for which the provision exists), and it was found that the FWHM depended upon the length of the cable used [21]. Three values are given below

Length of the cable (in cms.)	FWHM (ps)	FWTM (ps).
63.5	315	619.5
37.5	336	610.0
97.5	294	545.0

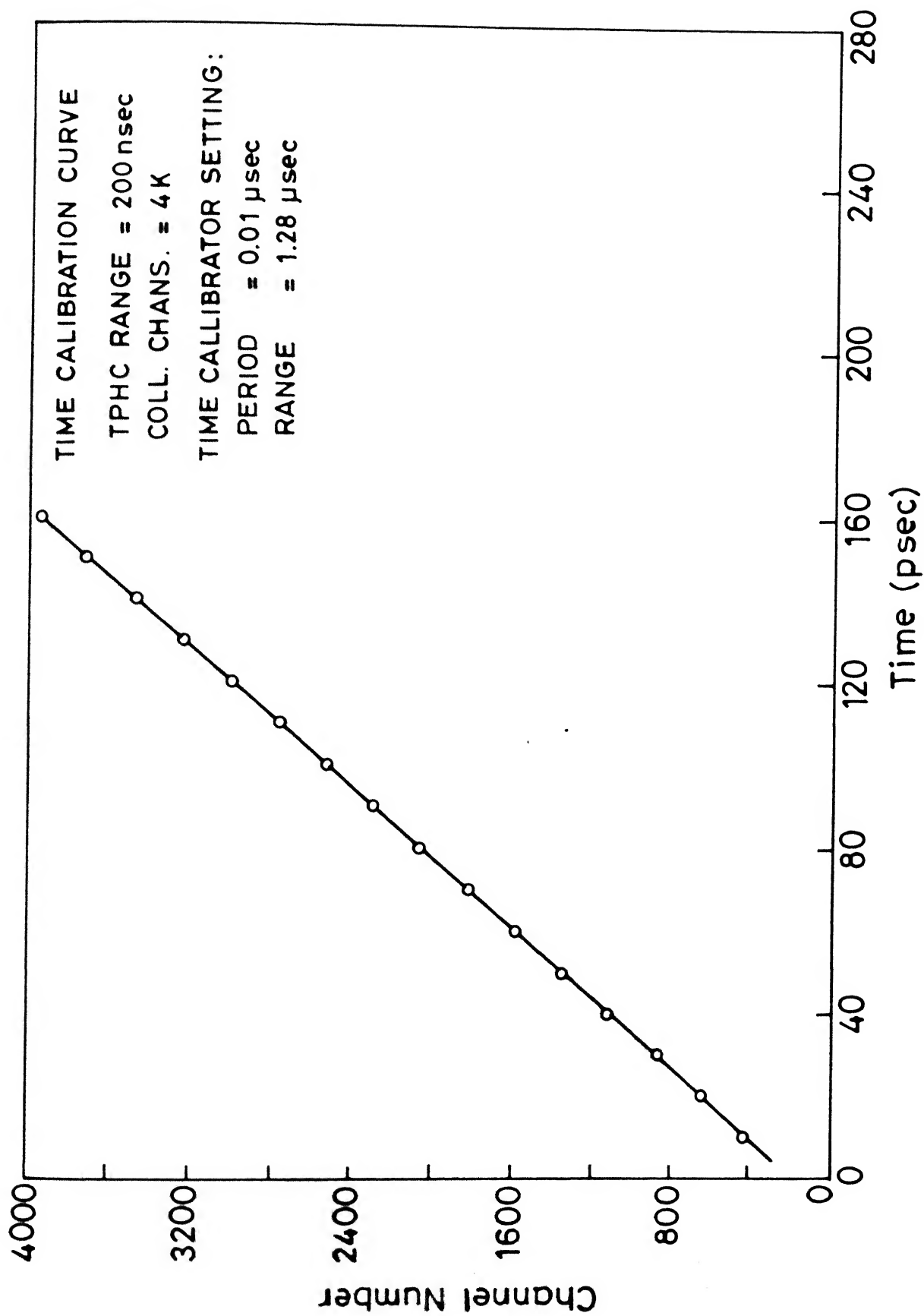
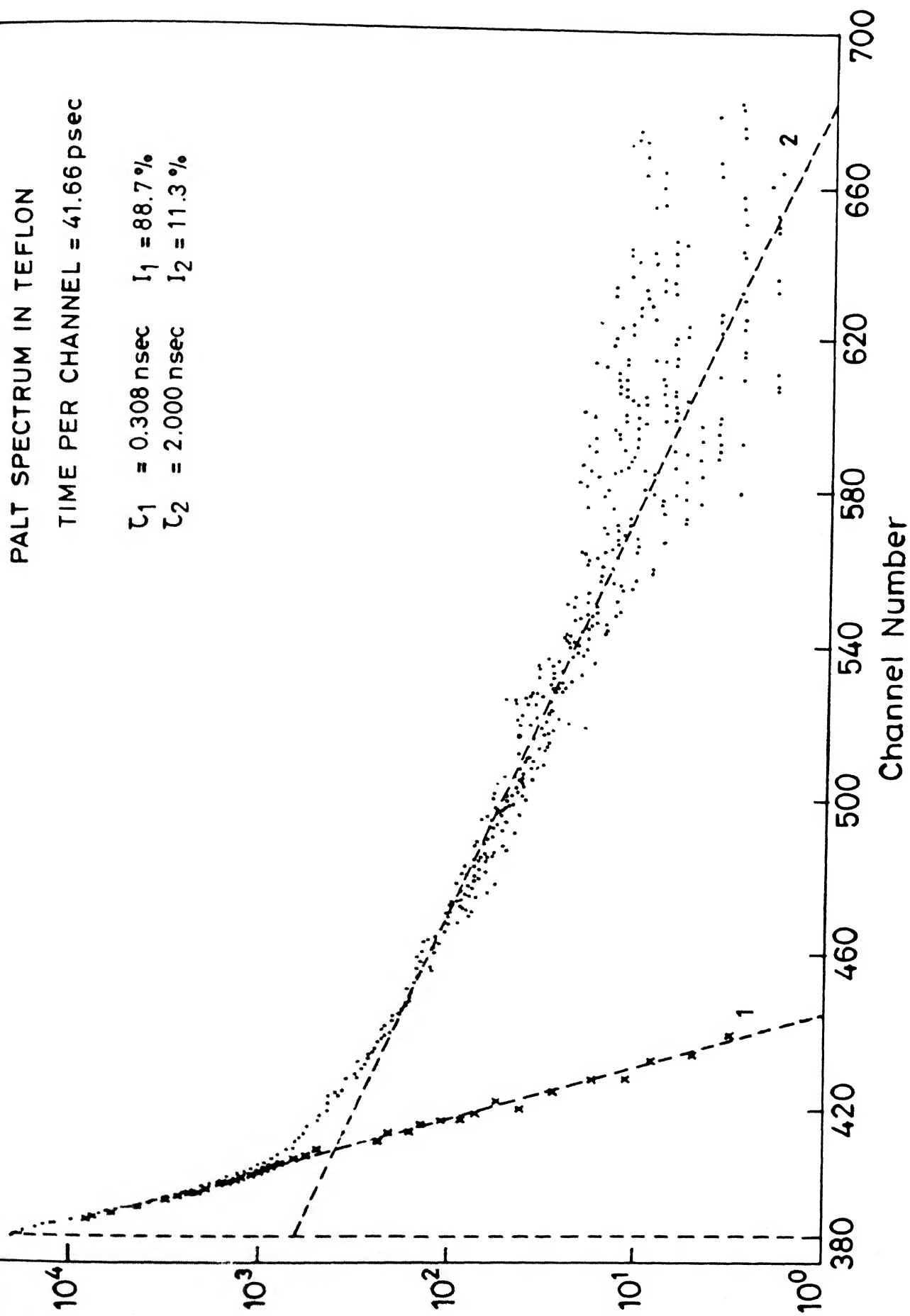


Fig.2.6. Time calibration line.

PALT SPECTRUM IN TEFLON

TIME PER CHANNEL = 41.66 psec

$\tau_1 = 0.308 \text{ nsec}$ $I_1 = 88.7\%$
 $\tau_2 = 2.000 \text{ nsec}$ $I_2 = 11.3\%$



2.5.4. POSITRON ANNIHILATION LIFETIME (PALT) SPECTRUM IN TEFLON.

The performance of the spectrometer for measuring lifetimes was tested by measuring the positron annihilation lifetime in teflon. Doing this we ensured that our time spectrometer gave values of one lifetime component and intensity comparable to that reported in the literature. The spectrum obtained in teflon is shown in Fig.2.7..

The values obtained for teflon are given in Chapter 3.

CHAPTER-3.

DATA ANALYSIS, RESULTS AND DISCUSSION.

3.1. INTRODUCTION.

In this chapter the methods of analysing the PALT data and the results of the lifetime for some of the systems studied are presented.

3.2. DATA ANALYSIS.

The lifetime spectrum of teflon or for that matter any sample is generally a convolution of two or more exponentials by the resolution function of the time spectrometer [22,23]. To extract the lifetime components from the spectrum obtained is an intricate process and standard computer programs are available for the purpose of such data analysis. A brief discussion on the nature of the analysis pattern in the standard programs will be presented later.

The mathematical representation of the lifetime spectrum is

$$I(t) = (\sum I_i e^{-\lambda_i t} + \text{background}) \quad (1)$$

where I_i is the intensity of the i^{th} lifetime component, λ_i is the inverse of the i^{th} lifetime, and where $i = 1, 2$ (or sometimes upto 3).

The data analysis was carried out in two ways

- 1) Graphically, to obtain a feeling about the steps involved in data analysis and to check the values.
- 11) Using programs POSITRONFIT and RESOLUTION.

Before discussing the above methods, a brief discussion on the nature and the origin of the background is presented.

3.2. 1. BACKGROUND.

NATURAL BACKGROUND.

The origin of this type of background [24] is due to cosmic ray showers and environmental radiation. This background is very low and therefore it is not necessary to take this into account in our experiment.

RANDOM BACKGROUND.

In the coincidence method employed in the time-to-pulse-height conversion, chance delayed coincidence may occur between the input pulses. If A is the counting rate and W_p (secs). is the pulse width, then the chance for one start pulse to produce a stop pulse is AW_p . Consequently the random coincidence counting rate is A^2W_p . Thus the random counting rate is A^2 /sec.. The true counting rate is proportional to A . Therefore for a high true to random ratio a weak source is preferred, but a very weak source lowers the efficiency of the counting system. Hence an optimum source strength is to be chosen. In our experiment a true to random ratio of $\sim 10^4:1$ with ^{22}Na was maintained.

The random background in the graphical method of analysis was found by taking the average over 120 channels immediately from that point where the longest lifetime component is negligible.

3.2.2. GRAPHICAL ANALYSIS.

In the graphical analysis for a two lifetime spectrum one follows the peeling off approach wherein the background is first subtracted from the main spectrum to get the longer lifetime component τ_2 . This longer lifetime component is then subtracted from the main spectrum to get τ_1 . The fit is done using the least squares fit (LSF) method for a straight line. All the components were then extrapolated to the zero time axis and the respective areas under each component was calculated. The ratio of this area to the total area gives the intensity of that particular lifetime component.

3.2.3. DATA ANALYSIS USING COMPUTER PROGRAMS.

In the computer program used by us [25-27] for the data analysis the lifetime spectrum is analysed by an iterative least-squares technique of semilinear Marquardt [28] type. The mathematical model is a sum of decaying exponentials convoluted with a Gaussian resolution function, to which a background is added. Fixed values can be imposed on any number of lifetimes and relative intensities. Correlation of the annihilation in the source is also taken into account.

The main program POSITRONFIT first proposed [25] in 1971 was modified in 1974 [26] and the version which is presently being used [27] was put forward in 1981. A brief mention of the salient features of the programs RESOLUTION and POSITRONFIT is given here.

3.2.3.1 RESOLUTION.

In the analysis of the positron lifetime spectrum it is important to use a precise description of the instrumental resolution function for a reliable extraction of the lifetime components in a spectrum. The program RESOLUTION is used to determine the resolution function. In the program the resolution function is defined as a sum of Gaussians, the centroids of which may be shifted with respect to one another to allow for asymmetrical resolution curves. The width and shifts of these Gaussians as well as the lifetimes and their intensities are the fitting parameters in the program. Constraints may be imposed on all fitting parameters (except time zero). The mathematical model in RESOLUTION is the same as that in POSITRONFIT.

The input of the spectrum data in the form of counts are to be fed in a specific format. A model input structure is shown in Annexure 1, however the details can be found in [27].

3.2.3.2 POSITRONFIT.

The program POSITRONFIT was first developed to extract the lifetime by least-squares analysis [25]. The mathematical representation of the spectrum is done using the following assumptions 1) in a measured spectrum the numbers in the channels fluctuate around a curve that is the sum of the constant background and a number of decaying exponentials which are smeared on account of the finite time resolution.

These smeared functions are determined by convoluting the exponentials with the resolution function of the measuring system. The count numbers obey Poisson distribution. 11) the resolution function is considered to be a Gaussian function. However this assumption was later modified twice [26] and [27] and in our data analysis we use the latest version [27] where the resolution function is determined from the program RESOLUTION described earlier.

The greatest advantage of the program however lies in its provision for the source correction and the possibility of a change in the number of lifetime components after the source correction has been applied. This becomes particularly useful in situations where the spectrum contains long-lived components which are otherwise completely removed with the subtraction of source components.

3.3 LIFETIME SPECTRUM - DATA COLLECTION AND ANALYSIS.

In our experiment we had taken up the sample of metallic glass for study, but before doing that a test spectrum in teflon was taken (as was mentioned in Chapter-2) to check if the setup was working properly. After this step a spectrum was taken in annealed copper to find out the source contribution in the spectrum obtained. The source contribution results from the annihilation of positrons in the foil holding the source. The source used by us is laid on a thin nickel foil.

In the next part a brief mention of the data collection and analysis in teflon and annealed copper is given. This will be followed by an introduction to metallic glasses after which the results of the findings in metallic glasses will be presented.

3.3. 1. PALT SPECTRUM IN TEFLON.

It was stated in section 2.5.4 of Chapter 2 that the performance of our time spectrometer was tested by taking a test spectrum in teflon. In this section the sample details and the final results are presented.

Two teflon pieces of 1 mm thickness were cut out of a cylindrical block of 20 mm diameter and the source was placed in between the two pieces, the combination in the form of sandwich geometry was placed in a sample holder made for the purpose.

In the first set of data collected it was observed that the background counts were being chopped off from the spectrum and were not recorded. This was rectified by increasing the resolving time in the fast coincidence unit to 40 ns from its previous setting of 20 ns. The spectrum collected with the resolving time as 40 ns was as expected. The results obtained with a spectrum recorded for 10 hrs. at a counts per second (cps) value of 22 counts per sec. are

Lifetime	Intensity.
$\tau_1 = 0.308 \text{ ns}$	$I_1 = 98.7\%$
$\tau_2 = 2 \text{ ns}$	$I_2 = 11.3\%$

These values were found to be of the same order as have been reported in the literature, however an exact match cannot be obtained because the purity of different samples is bound to be different.

3.3.2 LIFETIME SPECTRUM IN ANNEALED COPPER.

After the performance of the time spectrometer was found to be satisfactory the next step involved in the process of studying the lifetime of samples with this spectrometer was to find out the contribution of the annihilation of positrons in the source in the spectrum recorded. To do this we recorded the spectrum in a material which is known to have a single lifetime. The reason for doing so was that, if the recorded lifetime spectrum shows the presence of two lifetime components, then an inference can be drawn that there is a contribution from the source.

In our experiment we used copper annealed at 800°C as the reference. It is known that annealed copper is defect-free and its lifetime spectrum consists of a single component only. The PALT spectrum in annealed copper is shown in Fig.3.1.. The results obtained from the analysis of the copper spectrum is

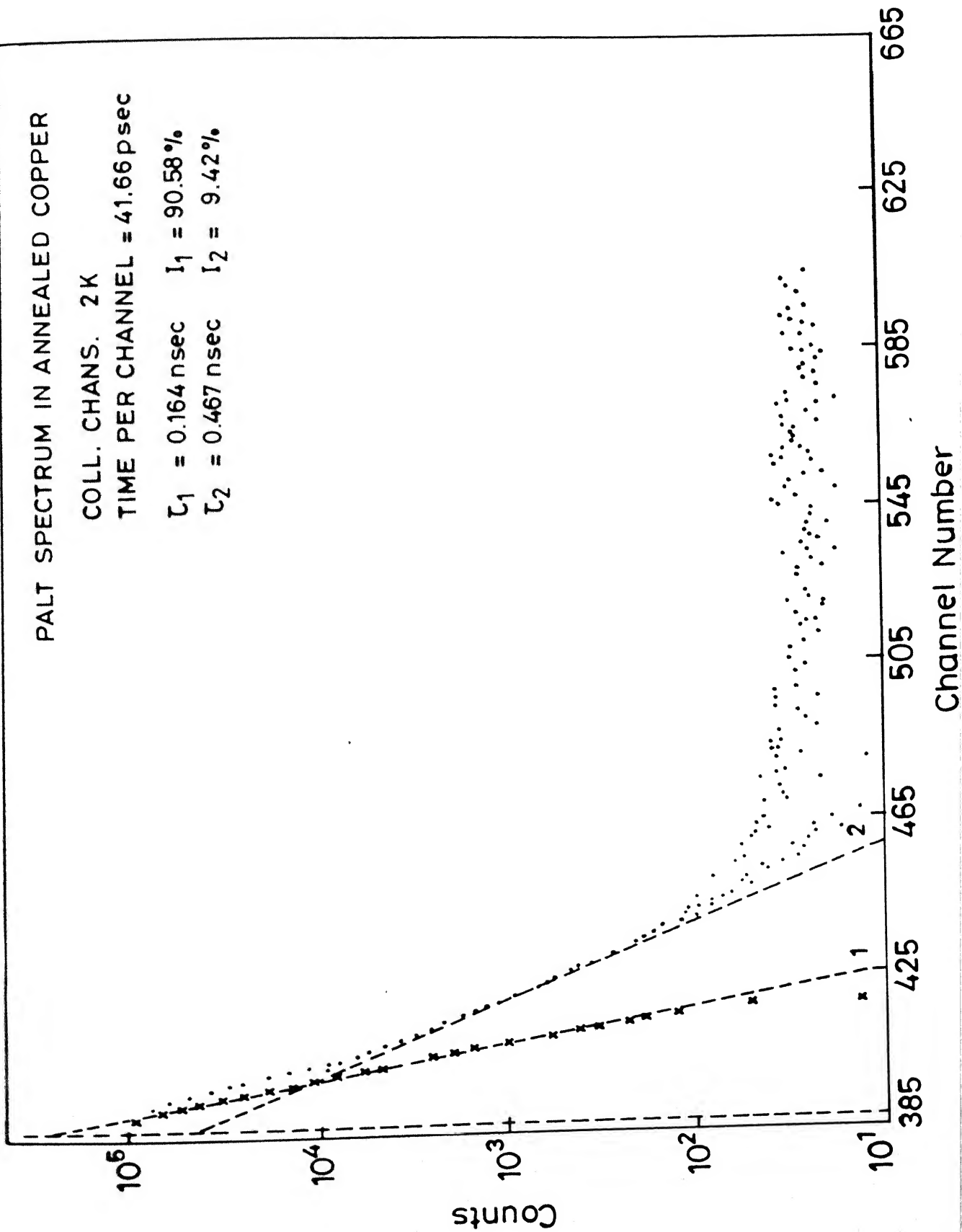
PALT SPECTRUM IN ANNEALED COPPER

COLL. CHANS. 2K

TIME PER CHANNEL = 41.66 psec

$\tau_1 = 0.164 \text{ nsec}$ $I_1 = 90.58\%$

$\tau_2 = 0.467 \text{ nsec}$ $I_2 = 9.42\%$



Lifetime	Intensity.
$\tau_1 = 0.164 \text{ ns}$	$I_1 = 90.58\%$
$\tau_2 = 0.467 \text{ ns}$	$I_2 = 9.42\%$

From the above result it is evident that there is a finite source contribution, which is the longer lifetime τ_2 but with a low ($\sim 10\%$) intensity. This factor has to be taken into account while collecting the spectrum with this source.

3.3.4 SPECTRUM IN A METALLIC GLASS SAMPLE.

With all the settings of the time spectrometer optimized and the source contribution calculated, we took up a sample of metallic glass for study. Before proceeding with the sample preparation and data analysis in this sample a brief introduction to metallic glasses with reference to their properties, types and preparation procedure is presented.

3.3.4.1 AMORPHOUS METALLIC ALLOYS.

The amorphous metallic alloys are metals and metallic alloys with no long range atomic order[29,30]. They are made by a variety of techniques, all of which involve rapid solidification of the alloying constituents from the glass or liquid phases. The solidification occur so rapidly that the atoms are frozen in their liquid configuration. The structural and the other properties indicate that nearest

neighbour or local order does exist in most amorphous metallic alloys but there is no trace of any long range atomic order, the correlation between atomic spacing is lost in about 5 atomic spacing. Due to their amorphous structure, the amorphous metallic alloys exhibit unique magnetic, mechanical, electrical and corrosion behaviour. They behave as very soft magnetic materials [31]; magnetic losses in high magnetisation amorphous alloys are lower than those measured in any other crystalline alloys. They are exceptionally hard and have a very high tensile strength. In some of the amorphous alloys the coefficient of thermal expansion can be made to be zero. The electrical resistivity is three to four times higher than those of conventional iron or iron nickel alloys. The amorphous alloys are also exceptionally corrosion resistant. There are two or possibly three technologically important classes of metallic amorphous alloy; the transition metal-metalloid (TM-M) alloys, the rare earth-transition metal (RE-TM) alloys and possibly the transition metal-zirconium or hafnium alloys.

The transition metal-metalloid alloys contain 80 atom percent iron, cobalt or nickel, with the remainder being boron, silicon, carbon, phosphorus or aluminium (either singly or jointly) and are typically prepared by rapid quenching of the melt. Other techniques like sputtering electrodeposition and chemical deposition have also been

used. The metalloid in the alloys helps in lowering the melting point, making it possible to quench the alloy through its glass temperature rapidly enough from the amorphous phase. The presence of the metalloids in the amorphous alloys also drastically alters the magnetic, mechanical and electrical properties of the alloys by donating electrons to the d-band. The presumed isotropic character of the TM-M alloys had been predicted to result in very low coercivities and hysteresis loss and high permeabilities; these properties are of significance for the alloy's application as soft magnetic material. The TM-Zr-Hf alloys, which contain about 10 atom percent zirconium or hafnium have properties which are similar to the TM-M alloys.

There are two important methods of preparation of metallic glasses[32]; in one the quenching is done so rapidly that there is insufficient time to nucleate and grow while in the other the vapour phase is deposited on a cold substrate so that the atoms during deposition do not have time to arrange themselves.

The RE-TM alloys are normally prepared by sputter deposition and have properties like low saturation magnetisation and high anisotropy perpendicular to the plane, which are specially suited for bubble-memory devices.

The rate of cooling \dot{T}_c (also known as the glass forming ability) required to form the metallic glass phase varies

from about 100 K/sec to 10^9 K/sec; the critical thickness x_c ranges from 1 mm down to 0.1 μm . However studies [33] have shown that the metallic phases can be formed at cooling rates of 10^6 K/sec or less in a wide variety of alloy systems.

The point of interest in amorphous alloys lies in the pursuit of explaining some properties which have unexpected features and ambiguities, for example, although the amorphous solids consist largely of random aggregates of atoms their densities are only slightly different from the density of crystals of the same composition. The broad theoretical question is; how does the amorphous atomic structure affect all the characteristics, i.e mechanical, electrical and chemical? Two types of structural models, 1) dense random packing of hard spheres (DRPHS) model and 11) cluster model have been used to describe the amorphous metallic structure.

3.3. 4.2 RESULTS OF PALT SPECTRUM IN METALLIC GLASS.

The metallic glass systems have been studied of late by several groups [34-37] the main form of study is to irradiate the sample and then study the migration of the defects in the sample and thereby try to predict the type of interaction that dominates the amorphous structure.

The metallic glass system that we had taken up for study was $\text{Fe}_{40}\text{Ni}_{38}\text{Mo}_4\text{B}_{18}$. Twelve pieces 15 mm by 15 mm in area and

60 μm in thickness were cut from a thin sheet of the same thickness, six pieces of the sample were then put together on the two sides of the source and this combination was placed in the sample holder. The spectrum was collected for 11 hrs. and is shown in Fig.3.2., the values obtained were

Lifetime	Intensity
$\tau_1 = 0.141 \text{ ns}$	$I_1 = 89.47\%$
$\tau_2 = 0.436 \text{ ns}$	$I_2 = 10.53\%$

But for the severe constraint of time, as a step for further investigation, we had plans to get our samples irradiated by heavy ions in the existing 2 MeV Van de Graff acclerator to look into the damage caused and to examine the effect it has on the positron lifetimes.

3.4. DISCUSSIONS.

In this experimental work we have setup a lifetime spectrometer using the fast-fast coincidence technique. The coincidence technique which is generally used in setting up a lifetime spectrometer is the slow-fast coincidence technique, where the slow channel performs the energy analysis and the fast channel performs the timing analysis, the slow coincidence output from the energy channel is used to gate the MCA in this method. The CFDD is used in the integral mode and the other channel uses the timing SCA for the purpose of energy selection. If two detected events fall within the

PALT SPECTRUM IN METALLIC GLASS $\text{Fe}_{40}\text{Ni}_{38}\text{Mo}_{14}\text{B}_{18}$

COLL. CHANS. 2K

TIME PER CHANNEL = 41.66 psec

$\tau_1 = 0.14 \text{ nsec}$ $I_1 = 89.47\%$

$\tau_2 = 0.43 \text{ nsec}$ $I_2 = 10.53\%$

Counts

Channel Number

selected energy range and if they are coincident within the resolving time of the coincidence unit a timing information is generated from the TPHC which is then fed to the MCA. But in a slow-fast coincidence system the dead time of the TPHC which varies between $5\ \mu\text{s}$ to $125\ \mu\text{s}$ imposes a count rate limitation [3.10]. The other source of count rate limitation lies in the charge preamplifiers where input count rate exceeding 100,000 counts per second can cause saturation in them.

In the fast-fast coincidence technique the CFDD generates the timing information and determines the energy range of interest simultaneously. If two detected events fall within the selected energy range and they are coincident within the preset resolving time of the coincidence unit, the TPHC is gated to accept only the delayed precise timing pulses. As the CFDD carries out a fast discrimination and the timing and energy information are taken from the same unit the limitations which exists in the slow fast coincidence system can be overcome. The fast-fast system can provide a good resolution with a strong source when a pile up gate is used in the configuration shown in Fig.3.3.

The resolution (FWHM) that we obtained with a dynamic range of 1:1 was 294 ps while the value with the ^{22}Na window was 348 ps. FWHM values of 189 ps with the fast-fast technique have been reported [39]. This value can be obtained in our

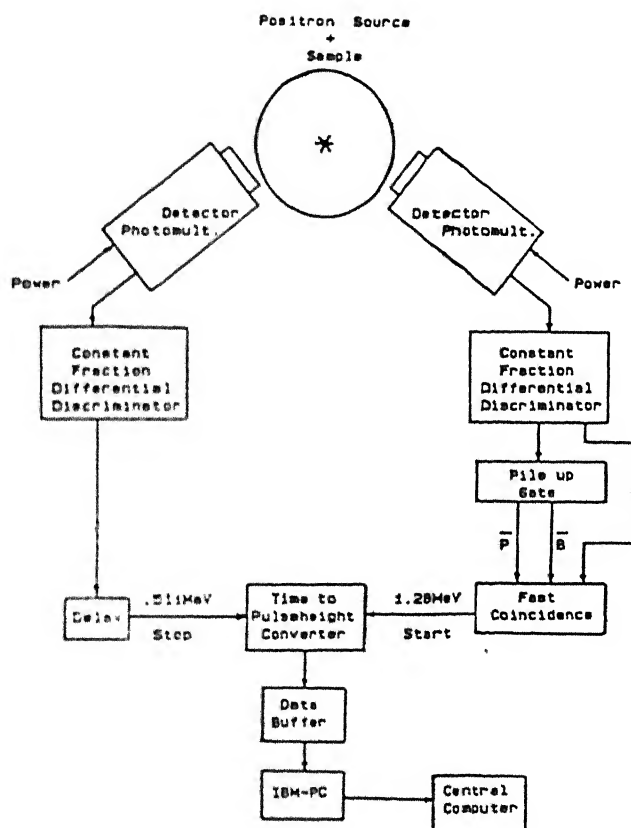


Fig. 3.3. A schematic diagram of time spectrometer using pile up gate.

setup also if we incorporate a pile up gate and optimise the size and shape of the scintillator. However it must be stated that most of the work reported in the literature on positron annihilation lifetime study have the FWHM of their system in the range of 260-370 ps.

LIST OF REFERENCES.

1. P.A.M.Dirac "The Principles of Quantum Mechanics"
Clarendon Press, Oxford (1947).
2. C.D.Anderson, Science, 76, 238 (1932).
3. P.M.S.Blackett and G.P.S.Occhialini, Proc. Roy. Soc.,
139, 699 (1933).
4. R.L.Garwin, Phys.Rev., 91, 1571 (1953).
5. G.E.Lee-Whiting, Phys.Rev.,97, 1157 (1955).
6. E.Ruark, Phys.Rev., 68, 278 (1945).
7. P.A.M.Dirac, Proc.Camb.Phil.Soc., 26, 361 (1930).
8. A.Ore and J.L.Powell, Phys.Rev., 75, 1696 (1949).
9. J.Green and J.Lee, "Positronium Chemistry", Academic
Press N.Y. (1964).
10. R.W Siegel, "Positron Annihilation Spectroscopy," pp.
393-495 in Ann. Rev. of Material Science, Vol. 10, R.A.
Huggens et al., eds.;Annual Reviews, Palo Alto, 1980.
11. Positrons in Solids Edited by P.Hautojärvi;
Springer-Verlag: Heidelberg, 1979, p-5.
12. Positrons in Solids; Edited by P.Hautojärvi,
Springer-Verlag: Heidelberg,1979, p-6.
13. Positrons in Solids, Edited by P.Hautojärvi,
Springer-Verlag: Heidelberg, 1979, p-4.
14. Positrons in Solids, Edited by P Hautojärvi,
Springer-Verlag: Heidelberg, 1979, p-7.

15. R.A.Ferrell, Rev.Mod.Phys., 28, 308 (1956).
16. Positrons in Solids, Edited by P.Hautojärvi,
Springer-Verlag: Heidelberg, 1979. p-8.
17. Positrons in Solids, Edited by P.Hautojärvi,
Springer-Verlag: Heidelberg, 1979, p-9.
18. S.Mantl and W.Triftshäuser, "Defect annealing studies on
metals by Positron Annihilation and Electrical
Resistivity Measurements," Phys. Rev. B, 17 (1978) pp.
1554-57.
19. Positron and Positronium Chemistry, Edited by
D.M.Schrader and Y.C.Jean, Elsevier: Amsterdam.
20. EG&G Ortec Model 462 Operating and Service Manual.
21. Proceedings of the Intrnational School of Physics "Enr
Fermi" (1981 :Varena Italy)
Positron Solid State Physics, Edited by W.Brandt and
A.Dupasquier, North Holland: Amsterdam, pp. 219-223.
22. Positrons in Solids, Edited by P.Hautojärvi,
Springer-Verlag: Heidelberg, 1979.
23. Proceedings of the Intrnational School of Physics "Enr
Fermi" (1981 :Varena Italy)
Positron Solid State Physics, Edited by W.Brandt and
A.Dupasquier, North Holland: Amsterdam, pp. 219-223.
24. J.Bell, S.J Tao and J.H.Green, Nucl.Instr. and Methods,
35, 213 (1965).
25. P.Kirkegaard and M.Eldrup, Computer Phys.Commun., 3, 240
(1972).

26. P.Kirkegaard and M.Eldrup, Computer Phys. Commun., 7, 401 (1974).
27. P.Kirkegaard and M.Eldrup, Computer Phys. Commun., 23, 307 (1981).
28. D.W.Marquardt, J. Soc. Ind. Appl. Math., 11, 431 (1963).
29. F.E.Lubrosky in Amorphous Metallic Alloys, ed. F.E.Lubrosky (Butterworths Monographs in materials :London).
30. R.W.Chan, Contemp. Phys., 21, 43 (1980).
31. P.Duwez and S.C.H.Lin, J. Appl. Phys., 38, 4096 (1967).
32. P.Duwez, R.H.Willenes and W.Klement,Jr., J. Appl. Phys. 31, 1136 (1960).
33. W.Klement, R.H.Willens and P.Duwez, Nature (London), 187, 869 (1960).
34. N.Shiotani, p 561, in
Proc. 6th Int. Conf. Positron Annihilation,
 Edited by P.G.Coleman, S.C.Sharma and L.M.Diana, North
 Holland (1982).
35. T.E.Jackman, J.R.Stevens, J.R.MacDonald, J.Fabian,
 P.sen and I.K.MacKenzie, in
4th Int. Conf. Positron Annihilation, Helsingor
 (1976) H8.
36. P.Moser, P.Hautojärvi, J.Yli-Kaupila, C.Corbel, in
Proc. of 6th Int. Conf. Positron Annihilation, Edited b
 P.G.Coleman, S.C.Sharma and L.M.Diana, North Hollar
 (1982) p 592.

37. J.Yli-Kauppila, P.Moser, H.Kunzi and P.Hautojärvi,
Appl.Phys. A27, 31 (1982).
38. Y.C.Jean and D.M.Schrader in Positron and Positronium
Chemistry, edited by D.M.Schrader and Y.C.Jean,
Elsevier:Amsterdam, (1988).
39. Michael D. Bedwell and Thomas J. Paulus in Proc. 5th
Int. Conf. Positron Annihilation (Japan, 1979), p-375.

1*** RESOLUTION INPUT ECHO ***

JOB 1 232

0

NEW

1 0 0

354

100.0

.0

24.0 4.19999E-02

20 120

NEW

INCLUDE

22 NOV 1990 METALLIC GLASS PURE Fe Ni B MO

72500.

6372.	28.	40.	36.	31.	38.	45.	45.	74.	103.
156.	236.	424.	804.	1459.	2886.	5235.	9750.	16263.	26241.
38902.	54805.	70730.	86718.	98991.	107268.	108100.	104125.	94070.	83413.
70261.	57042.	45827.	36158.	27751.	21990.	16899.	13469.	10506.	8303.
6723.	5525.	4456.	3705.	3050.	2627.	2306.	1885.	1651.	1434.
1237.	1141.	993.	841.	753.	706.	602.	573.	521.	494.
432.	391.	313.	312.	273.	276.	241.	220.	169.	191.
173.	139.	161.	135.	120.	123.	93.	83.	98.	97.
63.	70.	67.	59.	62.	55.	55.	49.	59.	56.
48.	36.	35.	30.	45.	40.	39.	43.	40.	42.
29.	30.	36.	29.	28.	25.	28.	26.	23.	20.
27.	23.	41.	23.	28.	26.	29.	24.	27.	15.
30.	30.	27.	21.	24.	20.	25.	21.	13.	24.
21.	22.	23.	14.	28.	26.	24.	23.	25.	20.
16.	20.	30.	15.	28.	22.	27.	19.	23.	21.
20.	22.	13.	12.	9.	23.	13.	17.	19.	15.
21.	15.	15.	19.	23.	20.	14.	21.	22.	21.
17.	23.	17.	24.	11.	16.	13.	25.	22.	17.
21.	22.	18.	24.	17.	15.	19.	24.	26.	20.
14.	15.	22.	18.	23.	18.	19.	17.	21.	19.
17.	19.	17.	27.	14.	17.	16.	15.	16.	19.
25.	22.	16.	24.	10.	14.	15.	13.	13.	19.
17.	21.	12.	23.	22.	19.	18.	18.	16.	20.
21.									

NEW

2 0 0

.46 .15

140 210

1R E S O L U T I O N ... VERSION FEB 82 ... DATE FOR THIS JOB r-w@-

GAUSSIANS 1 0 0
LIFETIMES 2 0 0

CONVERGENCE OBTAINED AFTER 10 ITERATIONS

PARAMETERS FOR SPECTRUM NO 6372

22 NOV 1990 METALLIC GLASS PURE Fe Ni B MO

TIME SCALE = .0420 NSEC/CHANNEL
SPECTRUM ANALYSIS STARTS IN CH. 20 AND ENDS IN CH. 120
BACKGROUND FIXED TO MEAN FROM CH. 140 TO CH. 210 = 19.085

INITIAL FWHM (NSEC): .3546
INIT.DISPLACEMENTS (NSEC): .0006

INITIAL LIFETIMES (NSEC): .4606 .1506

INIT.TIME-ZERO (CH.NO): 24.0006

VARIANCE OF THE FIT = 1.294 WITH STDEV = .146
 CHI-SQUARE = 121.61 WITH 94 DEGR OF FRDM
 SIGNIFICANCE OF IMPERFECT MODEL = 97.08 PCT

 RESOLUTION FUNCTION:
 FWHM (NSEC) .348
 STANDARD DEVIATIONS .001

INTENSITIES (PCT) 100.000

DISPLACEMENTS (NSEC) .037
 STANDARD DEVIATIONS

 LIFETIME COMPONENTS:
 LIFETIMES (NSEC) .436 .141
 STANDARD DEVIATIONS .006 .001
 INTENSITIES (PCT) 10.529 89.471
 STANDARD DEVIATIONS .383 .383

TIME-ZERO CHANNEL NUMBER 24.884
 STANDARD DEVIATION 37908.477

AREA CHECK AREA FROM FIT = 1.26564E+06
 AREA FROM TABLE = 1.26816E+06

NEWTON-RAPHSON PROCEDURE TO CALCULATE FORM PARAMETERS DID NOT CONVERG
 1 MATRIX OF TOTAL CORRELATIONS AMONG FREE PARAMETERS.
 THE ORDER IS: RELATIVE INTENSITIES, LIFETIMES, T0, FWHMS, DISPLACEMENTS.

1.000	-1.000	-.959	-.895	.571	.494	-.571
-1.000	1.000	.959	.895	-.571	-.494	.571
-.959	.959	1.000	.819	-.504	-.450	.504
-.895	.895	.819	1.000	-.694	-.684	.694
.571	-.571	-.504	-.694	1.000	.249	-1.000
.494	-.494	-.450	-.684	.249	1.000	-.249
-.571	.571	.504	.694	-1.000	-.249	1.000

1*** RESOLUTION INPUT ECHO ***

JOB-1 0